Science of the Total Environment 817 (2022) 152779

Contents lists available at ScienceDirect

Science of the Total Environment

journal homepage: www.elsevier.com/locate/scitotenv

Occurrence and *in vitro* toxicity of organic compounds in urban background $PM_{2.5}$

Jonas P. Wallraff [a,1], Florian Ungeheuer [a,1], Andrea Dombrowski [b], Jörg Oehlmann [b], Alexander L. Vogel [a,*]

[a] Institute for Atmospheric and Environmental Sciences, Goethe-University Frankfurt, Altenhöferallee 1, 60438 Frankfurt am Main, Germany
[b] Institute of Ecology, Evolution and Diversity, Goethe-University Frankfurt, Max-von-Laue-Str. 9, 60438 Frankfurt am Main, Germany

HIGHLIGHTS

- High-resolution mass spectrometry and *in vitro* toxicity assays applied on $PM_{2.5}$.
- The chemical composition of urban background $PM_{2.5}$ has a strong source dependency.
- Urban $PM_{2.5}$ exerts higher *in vitro* toxicity than $PM_{2.5}$ advected from an airport.
- Unspecific and specific toxicity correlate well with $PM_{2.5}$ mass concentration.
- Future work needs to identify the drivers for toxicity in urban PM.

GRAPHICAL ABSTRACT

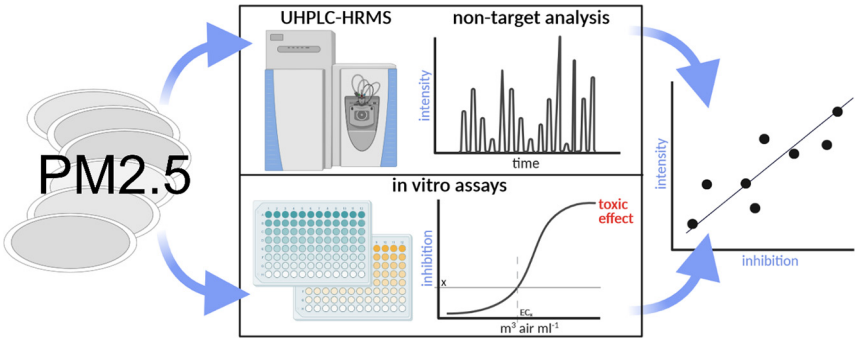

ARTICLE INFO

Article history:
Received 29 October 2021
Received in revised form 12 December 2021
Accepted 25 December 2021
Available online 8 January 2022

Editor: Jianmin Chen

Keywords:
Non-target analysis
Baseline toxicity
Microtox
AChE inhibition
Particulate matter
Aerosol

ABSTRACT

This study describes the chemical composition and *in vitro* toxicity of the organic fraction of fine particulate matter ($PM_{2.5}$) at an urban background site, which receives emissions either from Frankfurt international airport or the city centre, respectively. We analysed the chemical composition of filter extracts ($PM_{2.5}$) using ultrahigh-performance liquid chromatography coupled to a high-resolution mass spectrometer, followed by a non-target analysis. In parallel, we applied the bulk of the filter extracts to a Microtox and acetylcholinesterase-inhibition assay for *in vitro* toxicity testing. We find that both the chemical composition and toxicity depend on the prevailing wind directions, and the airport operating condition, respectively. The occurrence of the airport marker compounds tricresyl phosphate and pentaerythritol esters depends on the time of the day, reflecting the night flight ban as well as an airport strike event during November 2019. We compared the organic aerosol composition and toxicity from the airport wind-sector against the city centre wind-sector. We find that urban background aerosol shows a higher baseline toxicity and acetylcholinesterase inhibition compared to rural $PM_{2.5}$ that is advected over the airport. Our results indicate that the concentration and individual composition of $PM_{2.5}$ influence the toxicity. Suspected drivers of the acetylcholinesterase inhibition are i.e. organophosphorus esters like triphenyl phosphate and cresyldiphenyl phosphate, and the non-ionic surfactant 4-tert-octylphenol ethoxylate. However, further research is necessary to unambiguously identify harmful organic air pollutants and their sources and quantify concentration levels at which adverse effects in humans and the environment can occur.

1. Introduction

Air pollution is a significant worldwide environmental risk with adverse effects on human health, which are largely determined by fine particulate matter ($PM_{2.5}$, aerodynamic diameter < 2.5 μm) (Landrigan et al., 2018; Lelieveld et al., 2015; Lim et al., 2012). $PM_{2.5}$ enters the respiratory system

* Corresponding author.
E-mail address: vogel@iau.uni-frankfurt.de (A.L. Vogel).
[1] These authors contributed equally.

http://dx.doi.org/10.1016/j.scitotenv.2021.152779

via airways and can penetrate deep into the lung (Xing et al., 2016). Chronic exposure can lead to negative influences on mostly any organ (Schraufnagel, 2020; Schraufnagel et al., 2019). Lelieveld et al. (2019) estimate an annual excess mortality rate of 659,000 per year from air pollution in the European Union (EU-28), which largely can be attributed to $PM_{2.5}$ exposure. In the new air quality guidelines of the World Health Organization (WHO) the $PM_{2.5}$ limit has been reduced from 10 down to 5 μg m^{-3} (WHO, 2021). This limit is exceeded in many European regions (European Environment Agency (EEA), 2019).

In order to assess the health effects of ambient PM, a small fraction of anthropogenic organic pollutants is monitored in urban areas. These are usually polycyclic aromatic hydrocarbons (PAHs), and more rarely phthalate diesters and organophosphorus esters (OPEs). Both PAHs, as well as their transformation products, nitro-PAHs, are mutagenic and carcinogenic substances (Bandowe and Meusel, 2017; Guo et al., 2011; Kim et al., 2013). Phthalate diesters, mostly used as plasticisers, are suspected to exert a variety of toxic effects (*e.g.*, endocrine disrupting effects) in humans and animals (UBA (Umweltbundesamt), 2004, 2017). OPEs, such as triphenyl phosphate (TPhP) or tributyl phosphate (TBP) have numerous use cases *e.g.*, as flame retardants, plasticisers, or additives in lubrication and hydraulic oils, why they are found in both indoor and outdoor air (Reemtsma et al., 2008; Wong et al., 2018; Zhou et al., 2017). Many OPEs are hazardous. The specific mechanism of intoxication is the inhibition of the acetylcholinesterase (AChE) *via* phosphorylation, which can lead to cholinergic overstimulation resulting in headaches, emotional instability, confusion, as well as chronic diseases (Abou-Donia, 1981; Winder and Balouet, 2002).

However, there is still a lack of a holistic understanding of the chemical composition of urban organic aerosol (OA), and the number and identity of harmful chemicals that remain undetected is highly uncertain. In contrast, *in vitro* biotests of PM extracts always respond to the complex mixtures that are tested. Various studies show that particulate matter can induce oxidative stress, genotoxicity, DNA degradation, inflammation, and apoptosis, with harmful consequences on the respiratory and cardiovascular system (Arias-Pérez et al., 2020). The oxidative potential of airborne PM, as a metric for acute PM health effects (Bates et al., 2019), led to the recognition that anthropogenic emissions from residential wood burning and non-exhaust vehicular emissions are mostly associated with the oxidative potential concentration (Daellenbach et al., 2020). Further studies show that air pollution also exhibits detrimental effects on the central nervous system and increases the risk of dementia and neurodegeneration (Chew et al., 2020; Kanninen et al., 2020; Peters et al., 2019). Still, the molecular link to specific chemicals or chemical classes as toxicity drivers remains elusive, while there is evidence that the mass of PM alone cannot explain the variability of toxicological effects (Cassee et al., 2013; Rönkkö et al., 2021; Daellenbach et al., 2020).

In earlier studies, the Microtox assay with the autoluminescent bacterium *Aliivibrio fischeri* was used to examine the baseline toxicity of $PM_{2.5}$. The Microtox assay considers multiple toxicological effects that take place at the cellular level, such as log K_{OW}-dependent unspecific effects that include narcosis, uncoupling (disruption of the oxidative phosphorylation), and electrophilicity-based effects (Brack, 2003; Cronin and Schultz, 1998; Hermens et al., 1985; Lionetto et al., 2019; Schultz and Cronin, 1997). The assay is widespread in aquatic ecotoxicology and has previously been used for the examination of airborne particles (Lionetto et al., 2019; Roig et al., 2013). Lionetto et al. (2019) found a strong correlation between the bioluminescence inhibition in the Microtox assay and PM_{10} (aerodynamic diameter < 10 μm) concentration at an urban background in Southern Italy. They report a weak correlation between the baseline toxicity and the oxidative potential of PM_{10}, making it a valuable test system for airborne particles (Lionetto et al., 2019). In contrast, Roig et al. (2013) found no correlation between PM_{10} concentrations and the results obtained with the Microtox assay, concluding that only a few substances drive the toxicity.

The AChE inhibition of single chemicals or complex mixtures can be determined using the Ellman assay, in which acetylthiocholine, as an alternative enzyme substrate, is hydrolysed by AChE into thiocholine and acetate. The formed thiocholine can be photometrically determined using Ellman's reagent (Ellman 1961). To our knowledge, the AChE-inhibition assay has not yet been applied on organic extracts of atmospheric PM in order to determine the potential neurotoxic effects of organophosphates or other neurotoxic compounds.

To gain further insight about a potential composition-dependent toxicity, in this study we comprehensively characterised the chemical composition of organic $PM_{2.5}$ extracts and determined their toxic potential with the two *in vitro* assays; Microtox and AChE inhibition. The investigated samples were chosen to reflect the emissions of a large airport in contrast to air masses from a large city centre (urban background), which both can be considered as a of source of different organophosphates. $PM_{2.5}$ in airport direction was sampled during normal operation and during an airport strike event and before the Covid-19 pandemic.

2. Material and methods

2.1. Sampling site

Field sampling was conducted at the air quality monitoring station Frankfurt-Schwanheim, located 4 km north of the Frankfurt International Airport, Germany (Fig. 1). Frankfurt airport is the largest German commercial airport and counted over 70 million passengers in 2019 (Fraport, 2020). It is located 100 m above sea level at 50° 3′ 40″ N, 8° 33′ 51″ E.

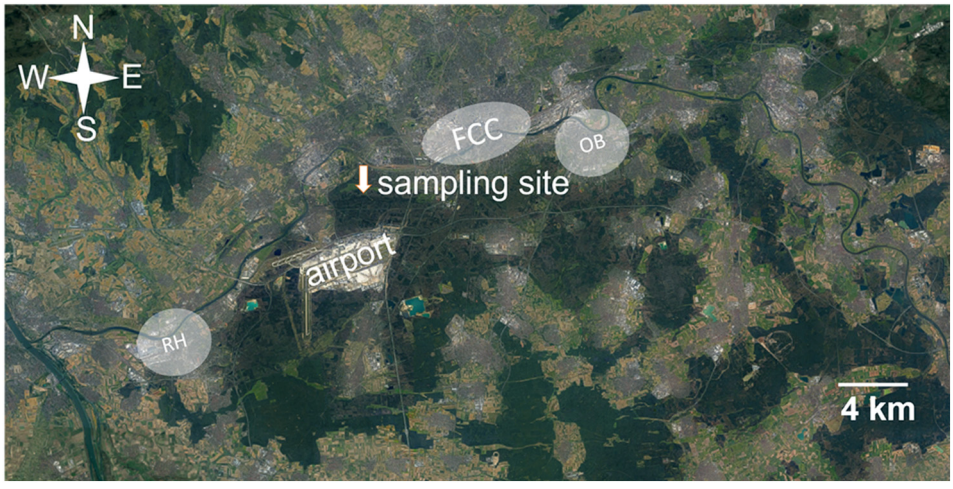

Fig. 1. Location of the air quality monitoring station Frankfurt-Schwanheim. It is located 4 km north of the Frankfurt International Airport. FCC – Frankfurt city centre, OB – city of Offenbach, Main, RH – city of Rüsselsheim (Bilder © 2021, Google,Bilder © 2021 TerraMetrics, Kartendaten © 2021 GeoBasis-DE/BKG (©2009)).

The main wind directions at the airport are south-southwest and northeast (HLNUG, 2018). South-southwest is the predominant direction. The monitoring station is located on a sports ground, the nearest street is in approximately 100 m distance. It is surrounded by the Frankfurt forest. The city centre of Frankfurt (FCC) is located roughly 4 km northeast of the station (Fig. 1). The district Niederrad and the residential area of Schwanheim are located 4 km east-northeast, and 2 km north-northeast, respectively. The city Offenbach (OB) lies 14 km east-northeast of the station, the city Rüsselsheim (RH) in a distance of 15 km southwest (Fig. 1). According to the Hessian Agency for Nature Conservation, Environment, and Geology (HLNUG) the air quality monitoring station Schwanheim has urban background characteristics (HLNUG, 2018). This is excepted by the lower burden with airborne pollutants due to the distance to inhabited areas (HLNUG, 2018). At south-southwesterly wind direction there is a rural emission background with low anthropogenic influence, with the exception of the airport. The station is representative for the emissions of highly frequented airports, overflights do not take place (HLNUG, 2018).

2.2. Sampling procedure

$PM_{2.5}$ was sampled during the 30th of October 2019 to the 9th of November 2019 using a High Volume Air Sampler (HVS) (Digitel DHA-80, Digitel Elektronik AG, Volketswil, Switzerland) loaded with baked-out (6 h at 450 °C) micro glassfiber filters with a diameter of 150 mm (Munktell MG 160, Ahlstrom-Munksjö, Helsinki, Finland). A sampling interval of 6 h per filter was chosen to illustrate the night flight ban at Frankfurt Airport, which applies from 23:00 to 05:00. The HVS was operated with a flow of 500 l min^{-1}.

After sampling, the filters were stored at −20 °C until further analysis. Three different sampling conditions were chosen, each reflecting specific wind directions. Filters that were taken during normal airport operation and main wind direction from south-southwest are marked as AN (Fig. 2). Filters assigned to condition AS were sampled during a Deutsche Lufthansa strike in November 2019 with comparable wind conditions as AN (Fig. 2). The city condition (C) includes filters that were taken during the main wind directions from north-northeast to east-northeast, reflecting an urban background from the city centre (Fig. 2). For every condition four filters were analysed, one assigned to nighttime (23:00–05:00) and three sampled at daytime (Table 1). An unsampled filter, which was treated just as the samples, was stored inside the HVS for a couple of days and served as field blank for both chemical analysis and toxicity testing.

2.3. Sample preparation

The sampled filter area used for analysis was 154 cm^2. A whole filter was cut into small pieces using pre-cleaned ceramic scissors. The pieces were transferred into a 30 ml glass vial. For the extraction of organic compounds, a total of 20 ml distilled dichloromethane (DCM) was used in a two-step extraction. In the first step, filters were covered with 15 ml DCM and extracted on an orbital shaker (KS 15-A, Edmund Bühler GmbH, Bodelshausen, Germany) for 20 min at 300 rpm. Afterwards, the solvent extract was filtered using a solid phase extraction (SPE) cartridge made of glass. It was loaded with a filter punch that retained particles of ≥1.2 μm (Munktell MG 160) and fitted with a steel pin. The second extraction step consisted of the same procedure but was carried out using only 5 ml of DCM. Thereupon, the pooled extract of about 15 ml was evaporated near dryness under a gentle nitrogen stream and at 35 °C. The remaining extract was transferred into a 1 ml glass vial. The extraction glass was rinsed with a small amount of DCM, which was pooled with the extract. The extract was then evaporated to dryness. The residue was taken up in 85 μl of MeOH:H_2O (50:50) (see 2.5 Chemical analysis for used chemicals) and used for *in vitro* testing. All analyses were carried out within 3 weeks after sample preparation. For the chemical analysis of $PM_{2.5}$, aliquots of 5 μl from the *in vitro* extracts were taken and diluted 1:20 by MeOH:H_2O (50:50). The remaining *in vitro* extract (80 μl) was further diluted for triplicate and quadruplicate *in vitro* analysis. Hence, the procedure ensures identical sample extraction conditions for both the *in vitro* and organic-chemical analysis.

Table 1
List of analysed samples.

	Normal airport operation (AN)		Airport strike (AS)		City (C)	
	Sample #	Time	Sample #	Time	Sample #	Time
Nighttime	AN27	23:00–05:00	AS31	23:00–05:00	C5	23:00–05:00
Daytime	AN19	11:00–17:00	AS29	11:00–17:00	C7	11:00–17:00
	AN24	17:00–23:00	AS30	17:00–23:00	C4	17:00–23:00
	AN26	17:00–23:00	AS28	05:00–11:00	C3	11:00–17:00

2.4. In vitro testing

The sample-extracts (four per sampling condition) were tested for baseline toxicity, applying the Microtox assay according to Escher et al. (2008) and neurotoxic effects using an AChE inhibition assay. Microtox assays with *A. fischeri* cover effects altering the bacterial energy metabolism (Brack, 2003). The assay provides insight about the unspecific toxicity as multiple stressors may inhibit the metabolism of *A. fischeri* leading to decreased bioluminescence (Escher et al., 2014; Völker et al., 2017). The decrease in bioluminescence reflects the cellular metabolic status as determinant for the toxicity (Abbas et al., 2018). As a specific assay targeting neurotoxicity, the AChE inhibition assay originally described by Ellman et al. (1961) was used. The assay aims to examine potential neurotoxic effects caused by AChE inhibitors such as organophosphorus compounds (Eyer, 1995; Winder and Balouet, 2002).

2.4.1. Baseline toxicity

The baseline toxicity was determined using the bioluminescent bacterium *A. fischeri* following the procedure described in Escher et al. (2008) and was based on the ISO-guideline (ISO 11348-3:2007). $PM_{2.5}$ extracts and controls including 3,5-dichlorophenol as positive control were serially diluted (1:2) obtaining eight concentrations for each sample. For the

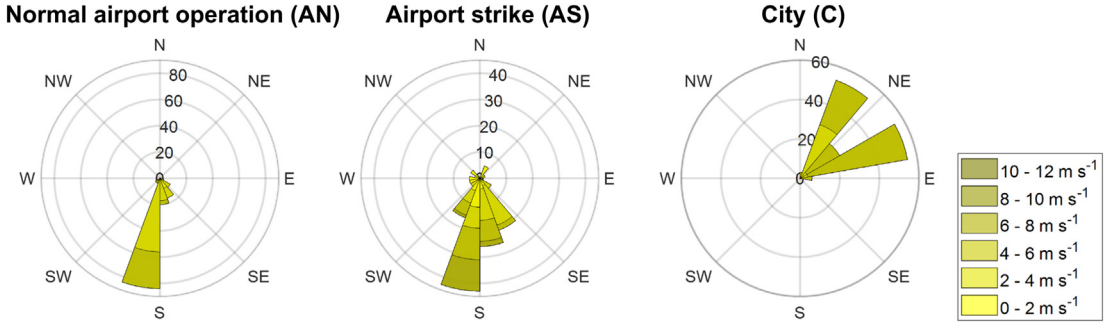

Fig. 2. Wind roses indicating the wind directions and speed of the examined filters assigned to the three sampling conditions. All filter samples were taken during 30.10.2019 to 09.11.2019. Data provided by the meteorological station at Frankfurt airport (ICAO-Code: EDDF) of the Deutscher Wetterdienst (DWD).

extracts these dilutions refer to 0.35 to 47 m^3 air ml^{-1}. The diluted sample solutions (100 μl) were added to 50 μl of bacterial suspension. The luminescence emitted by *A. fischeri* was measured prior to and 30 min after sample addition using a microplate reader (Tecan Spark 10 M, Tecan Group, Männedorf, Switzerland). Each sample was tested in three independent experiments including one technical replicate. The results were corrected for the inhibition caused by the negative controls (bacterial solution without any present inhibitor) resulting in a relative inhibition rate (%). By pooling the triplicates, a mean relative inhibition was derived for each sample. Based on this, an effective concentration (EC_{20} ± confidence intervals (CI) in m^3 air ml^{-1} reflecting a decrease in light emission of 20%) was calculated using a nonlinear regression model. The upper plateau was constrained to 100% luminescence inhibition, the lower plateau to the inhibition caused by the field blank, respectively.

2.4.2. AChE inhibition

The assay according to the protocol by Ellman et al. (1961) was used. Further alterations were made to adapt the assay to 96-well plates as described by Sigma-Aldrich (2018). 10 μl positive control (0.1 mM paraoxon-methyl, PESTANAL®, ≥ 98% purity, Sigma-Aldrich, St. Louis, Missouri, USA), negative control (0.4 units ml^{-1} AChE from *Electrophorus electricus*, Sigma-Aldrich) or sample, and 90 μl AChE (0.4 units ml^{-1}) were added to a 96-well plate and diluted 1:2 column-wise, obtaining eight concentrations for each sample. For the extracts these dilutions refer to 0.4 to 53 m^3 air ml^{-1}. After incubation on a platform shaker (Titramax 1000, Heidolph Instruments GmbH & Co. KG, Schwabach, Germany) for 5 min at 450 rpm the reaction was started by adding 150 μl of the reaction mix consisting of 5,5′-dithio-bis-(2-nitrobenzoic acid) (30 μM, ≥ 98% purity, Sigma-Aldrich) and acetylthiocholine iodide (600 μM, ≥ 98% purity, Sigma-Aldrich) dissolved in phosphate buffer (1.5 M, pH 7.2) (see Supplementary Information (SI), Table S1). The increase in absorbance was immediately measured at 412 nm over 6 min in intervals of 15 s using a microplate reader (Tecan Spark 10 M, Tecan Group). Each sample was tested in four independent experiments including one technical replicate. Only samples showing a linear absorbance increase ($r^2 \geq 0.9$) in the initial reaction phase of the kinetic were used for further data evaluation. The inhibition rate was calculated as described by Sigma-Aldrich (2018) where ΔA_{sample} is the increase in absorption for each individual sample and $\Delta A_{NCpooled}$ reflects the averaged increase in the negative controls without a present inhibitor (Eq. (1)). Based on the inhibition rate an EC_{25} pooling the quadruplicates was calculated for each sample using a nonlinear regression model. The upper plateau was constrained to 100% AChE inhibition, the lower one to 0%, respectively.

$$Inhibition\ [\%] = \frac{1 - \Delta A_{sample}}{\Delta A_{NCpooled}} \times 100 \quad (1)$$

2.5. Chemical analysis of organic PM fraction

The chemical composition of $PM_{2.5}$ was examined using an ultra-high performance liquid chromatograph (UHPLC; Vanquish Flex, Thermo Fisher Scientific, Waltham, Massachusetts, USA) coupled to a quadrupole-Orbitrap hybrid mass spectrometer (Q Exactive Focus, Thermo Fisher Scientific). The chromatographic separation of compounds was carried out on an Accucore™ C_{18} column (150 mm × 2.1 mm; 2.6 μm solid-core particles, Thermo Fisher Scientific) operated in gradient mode with a constant flow of 400 μl min^{-1} and heated to 40 °C (still air). Ultrapure water (solvent A) (Millipak® Express 40: 0.22 μm, Millipore; Milli-Q® Reference A+, Merck, Darmstadt, Germany) and Methanol (solvent B) (Optima™ LC/MS grade, Thermo Fisher Scientific), both acidified (*v*/v 0.1%) with formic acid (LiChropur® ≥ 98% purity, Merck), were used as mobile phase. The chromatographic separation started with 5% solvent B, maintained for 1 min. Within 12 min the amount of solvent B was increased to 95% and held for 2 min. Subsequently, the starting conditions were restored by decreasing solvent B to 5% within 2 min, allowing the system to equilibrate for 3 min before the next run. Altogether, one chromatographic run lasted 20 min. The sample (5 μl) was injected using an autosampler thermostated at 15 °C. Samples were ionised *via* heated electrospray ionisation (HESI) and measured in the positive ionisation mode over a range of mass-to-charge ratio (*m/z*) 50–750. The mass resolving power was ~70 k at *m/z* 200. The capillary voltage was set to 3.5 kV, the capillary temperature was at 300 °C. The sheath gas was set to a flow of 50 psi (nitrogen), the aux gas flow rate was set to 10 psi (nitrogen) with an aux gas temperature of 350 °C. The Orbitrap instrument was operated in discovery mode to gain further insight into the fragmentation of single compounds. In this mode, fragmentation spectra of the highly abundant signals are recorded by estimating a peak apex during acquisition of the chromatogram. Prior to the measurements, the MS was calibrated using an external calibration solution (Pierce™ LTQ Velos ESI positive ion, Thermo Fisher Scientific) obtaining a mass accuracy of better than 2 ppm.

2.6. Non-target analysis and data filtering

The full-scan MS spectra were analysed by the non-target analysis software Compound Discoverer (CD) (version 3.2.0.421, Thermo Fisher Scientific) as described by Ungeheuer et al. (2021). CD was already tested against the non-target analysis software MZmine2 (Vogel et al., 2019). Briefly, CD identifies compounds and determines the molecular composition based on the measured exact mass, isotopic signature, MS/MS fragmentation patterns and compares measured MS/MS fragmentation spectra with a MS/MS database (mzcloud.org, last access: 12th January 2021). For the detection of compounds, a mass tolerance of 5 ppm was used, and further constrained to 2 ppm for the formula prediction. The analysis results were filtered with Matlab (R2019b, MathWorks, Natick, Massachusetts, USA) by the following requirements: the minimum sample-to-blank ratio (s/b) of a compound had to be five, the minimum area 1×10^5 counts and the minimum retention time 0.7 min (deadtime of the used column was 0.6 min). The peak areas of each sample were background corrected by subtracting the related peak area of the field blank. Minimum element counts of C_1, H_1 and maximum counts of C_{90}, H_{190}, Br_3, Cl_4, N_4, O_{20}, P_1, S_3 were used. The obtained molecular formulae of the organic molecules were categorised into compound classes according to their elemental composition (CHO, CHN, CHNO, CHOS, CHNOS, or CHOP). Compounds to which a molecular formula could not be assigned were classified as 'other'. To compare the different sampling conditions, the summed area of each compound class was calculated. For the comparison of two conditions, an unpaired *t*-test with Welch's correction using the software GraphPad Prism (Version 5.01, GraphPad Software, San Diego, California, USA) was performed. A *p*-value <0.05 was considered as statistically significant and is indicated by ★.

2.7. Measurement of $PM_{2.5}$ concentrations

The $PM_{2.5}$ concentrations (in μg m^{-3}) were continuously measured using a hybrid particulate mass monitor (SHARP 5030, Thermo Fisher Scientific) that utilizes nephelometry and β-absorption for real-time measurements of $PM_{2.5}$. For each sampling interval referring to one sample and 6 h, we averaged the $PM_{2.5}$ concentrations based on hourly $PM_{2.5}$ concentration values. The data was provided by the HLNUG and is available to the public (HLNUG (2019), last access: 7th July 2021). We correlated the averages with the summed signal intensity of the detected organic molecules using the software GraphPad Prism. For the linear correlation a p-level of <0.01 was considered as a statistically significant correlation.

2.8. Statistical analysis of bioassay data

The software GraphPad Prism was used for nonlinear regression and statistical analyses of the *in vitro* assay data. Statistical differences between the EC-values were obtained by comparison of the 95% confidence intervals. Non-overlapping CIs were considered statistically significant at a p-level of 0.05. We used the Pearson correlation coefficient to gain insight

about statistical relationships between the chemical composition and *in vitro* toxicity. Each samples' luminescence and AChE inhibition (%) caused by the highest analysed concentration in the dilution series of the corresponding assay was tested for linear correlations with the summed signal intensities of each compound class. Further, it was tested with the overall signal intensities for all detected compounds. A p-level < 0.01 was considered as a statistically significant correlation. The correlations were compared by their coefficient of determination (r^2).

3. Results

3.1. In vitro toxicity

3.1.1. Baseline toxicity

The baseline toxicity of the organic $PM_{2.5}$ extracts was evaluated by the Microtox test. For 75% of the examined samples an effect concentration of EC_{20}, which reflects a luminescence inhibition of 20%, could be calculated. The remaining samples exerted too low toxicity on *A. fischeri* to calculate an EC_{20}. The obtained EC_{20} values ranged from 24.7 to 57.1 m^3 air ml^{-1}. Individual values with corresponding 95%-CIs are given in Fig. 3A and the SI, Table S2. The highest luminescence inhibition was found in the samples from group C (C5 and C4) (Fig. 3). In this group, C4 had the lowest EC_{20} (24.7 (20.2 to 30.3) m^3 air ml^{-1}). This was significantly lower than AN27, AN26, AS28 and C3 ($p < 0.05$). Notably, samples with no calculable EC_{20}, and therefore no observed baseline toxicity, stemmed from groups AN and AS, while the highest inhibiting samples were all from group C. City samples excluding C3 had an EC_{20} of approximately 30 m^3 air ml^{-1}, whereas for samples taken during normal airport operation and strike, the values were about twice as high indicating a considerably lower baseline toxicity.

3.1.2. AChE inhibition

The neurotoxicity of the organic $PM_{2.5}$ extracts was examined by the evaluation of their AChE inhibition. The two highest test concentrations of each quadruplicate had to be excluded from the EC calculation due to high activity in the field blank (see SI, Fig. S1). The quadruplicates inhibition (%) for each concentration were tested for outliers with Grubb's outlier test according to Barnett and Lewis (1994). Outliers were excluded from the analysis. An EC_{25} was obtained for all but one sample, individual values and their 95% CIs are given in Fig. 3B and the SI, Table S2. The highest inhibition was obtained in samples of group C (Fig. 3). Samples from AN had lower values than those from AS. One sample that showed no AChE inhibition stemmed from group AN (AN19). The calculated EC_{25} values ranged from 1.39 to 11.2 m^3 air ml^{-1}. The highest inhibition of AChE was observed in samples that were taken during wind from north-northeast to east-northeast and daytime (C3 and C4), the lowest during airport strike and daytime (AS29 and AS30). AS29 had an EC_{25} of 11.2 m^3 air ml^{-1}. The value was significantly higher than all other obtained values ($p < 0.05$). The highest overall AChE inhibition was observed in the daytime sample C4. It had an EC_{25} of 1.39 m^3 air ml^{-1}, no overlapping CI with all samples but C3, and about a ten times lower EC_{25} than that of the least inhibiting sample AS29. Under normal airport operation, the largest inhibition was obtained for AN27. It had overlapping CIs with the other samples from AN and AS28, AS31, C5, C3, and C7. EC_{25} values of AS28 and AS31 were significantly lower than those of AS29 and AS30 ($p < 0.05$). Notably, the lowest EC_{25} and therefore highest inhibition for samples taken during the strike is reflected by the night-time sample AS31.

3.2. Organic aerosol molecular composition

The non-target screening detected a total of ~1600 different organic compounds within all analysed samples in the positive electrospray ionisation mode. Thereof, approximately 460 compounds showed at least fivefold higher signal intensities than the field blank. Airport marker compounds were detected in samples of both airport operation conditions and during day- and night-time. For a better graphical comparison between the sampling conditions, all samples of each condition were averaged (AN, AS, and C), and the organic molecular pattern is displayed by retention time against molecular weight (MW) (Fig. 4), Kroll-diagram (SI, Fig. S2), and Kendrick mass defect (KMD) against MW (Fig. 4). The KMD was calculated as described by Kendrick (1963) to identify homologous series of hydrocarbons with all homologues appearing plotted on a horizontal line. Every circle represents a single compound assigned to one of the seven compound classes. Their colouration depends on the assignment to one of the individual compound classes. The area of each circle is proportional to the signal intensity of the detected compound. We use the compound identification levels for HR-MS as suggested by Schymanski et al. (2014). All namely mentioned compounds are determined based on a minimum confidence level of two and marked accordingly (level 1: confirmed structure by reference standard; level 2: probable structure by library spectrum match) (Schymanski et al., 2014). The corresponding MS/MS spectra and chromatograms can be obtained from the SI. The compound dibutyl phthalate and its fragmentation product were excluded from the fingerprints due to their high signals in the field blank and its ubiquitous use as a plasticiser and cosmetic product (Benson, 2009). For some compounds, CD falsely interpreted ion signals of the measured ion $[M + Na]^+$ as $[M + H]^+$. This led to an overestimation of detected compounds since two to three additional false formulas with higher m/z than their parent molecular ion were suggested for each affected compound. These artifacts were filtered out based on the same retention time and exact mass difference between sodium and hydrogen.

Both scatter plots for normal airport operation (AN) and airport during strike (AS) show a similar molecular fingerprint, while the city condition

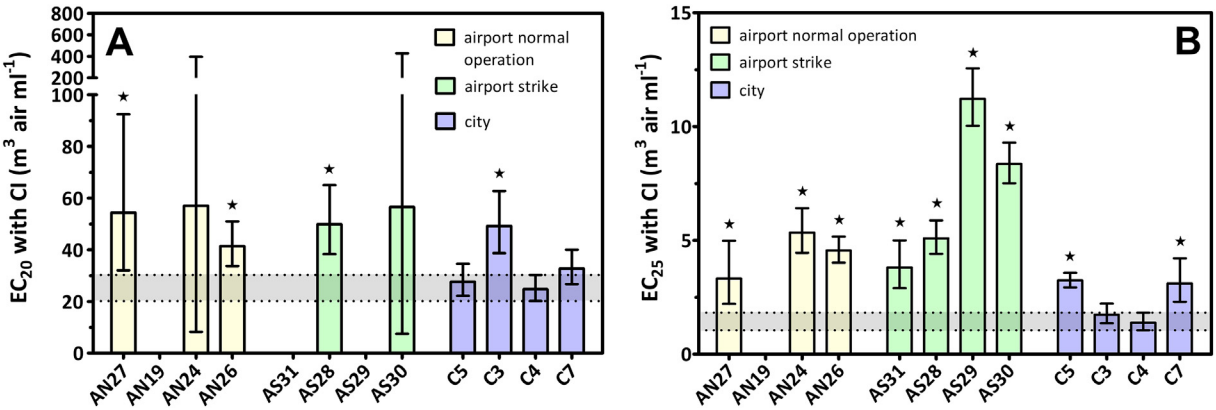

Fig. 3. Results of the Microtox and AChE inhibition assay. EC values are given with 95% confidence interval (CI) for baseline toxicity assessed *via* Microtox test (A, $n = 3$) and AChE inhibition (B, $n = 4$). In cases where a corresponding EC could not be calculated, the column is left out blank. The grey area indicates the interval of confidence of the sample with the highest activity, C4. Significant differences between C4 and the other samples at a *p*-value of <0.05 are indicated by ★ (CI comparison).

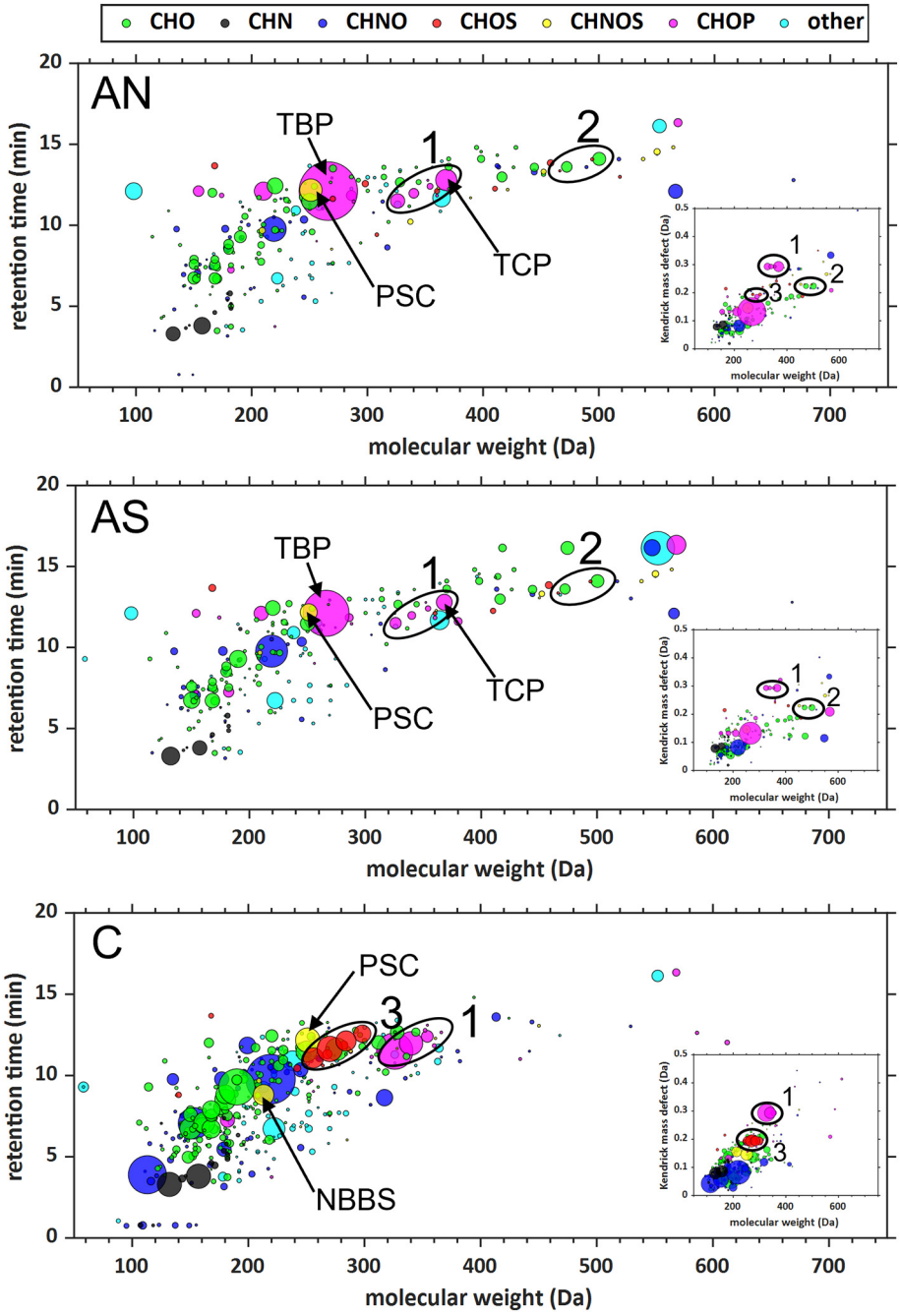

Fig. 4. Retention time against molecular weight (MW) and Kendrick mass defect plots based on the average of all samples belonging to a certain sampling condition. Three homologous rows were identified: 1 Homologues of organophosphate ($C_{18}H_{15}O_4P$ to $C_{21}H_{21}O_4P$), TCP is absent in C. 2 Pentaerythritol esters $C_{25}H_{44}O_8$ and $C_{27}H_{48}O_8$, 3 Homologous row of CHOS compounds present in C ($C_{16}H_{16}OS$ to $C_{19}H_{22}OS$) and AN ($C_{17}H_{18}OS$ and $C_{19}H_{22}OS$). Prosulfocarb (PSC) was present in all groups, N-butylbenzenesulfonamide (NBBS) only in C. AN – normal airport operation, AS – airport strike, C – city.

(C) clearly shows a distinct pattern (Fig. 4). We observed the highest number of different compounds and overall signal intensities in the city-condition samples. The summed intensities for all compounds detected in C were significantly higher than in AN (Welch's *t*-test, $p = 0.0251$) and AS ($p = 0.0257$) (Fig. 5). The samples C4 and C5 had the largest signal intensity of all detected compounds in total, AN19 and AS31 the lowest. The airport samples consisted mostly of CHO, CHNO, and CHOP compounds with CHO and CHOP showing the highest intensities. Under city-condition, the highest summed signal intensities were observed in the classes CHO and CHNO. The summed signals of these compound classes were two to four times higher than under both airport conditions. Compared to the city samples, we found higher summed intensities of phosphorous-containing (CHOP) organic compounds in the airport samples. Among the highest signals we identified the organophosphorus compounds tributyl phosphate (TBP, level 1), tricresyl phosphate (TCP, level 1), and dibutyl phosphate (level 2), which is likely generated in the ion source *via* fragmentation of tributyl phosphate. During the airport strike period, a greater heterogeneity in the largest detected compound-signals was observed. Two of them were assigned to the CHOP (tributyl phosphate and $C_{33}H_{61}O_5P$) and one to the CHNO class ($C_{14}H_{21}NO$). Among the highest signals in the city samples, we observed nitrogen-containing compounds (*e.g.* $C_6H_{11}NO$, $C_{19}H_{15}NO$, and $C_{14}H_{21}NO$), which are no organonitrates but rather secondary and tertiary amines that are likely directly emitted and not formed *via* secondary formation.

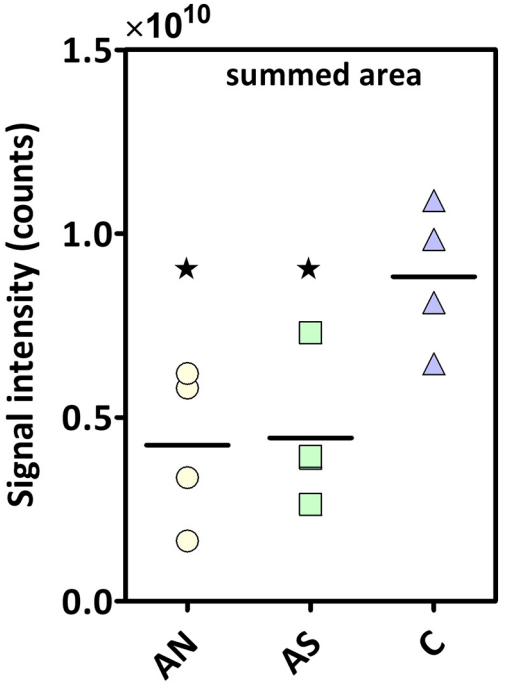

Fig. 5. Comparison between the summed signal intensities of all compounds with a signal to blank ratio higher than five. There is no significant difference between the summed intensity of AN and AS. Samples from C have significantly higher summed areas than AN and AS. Significant differences of $p < 0.05$ are indicated by ★ (unpaired *t*-test with Welch's correction).

Across all samples we detected 195 compounds of the CHO class. Thereof, 95 were found in AN, 100 in AS and 170 in C. The summed signal intensities of CHO for AN and AS were approximately the same, whereas C had at least twofold and significantly higher intensities than AN ($p = 0.0406$) and AS ($p = 0.0499$) (Fig. 6). The samples C4 and C5 had the largest summed signal intensity, sample AN19 and AS31 the lowest (Fig. 7). The CHO class of C predominantly consisted of molecules with an MW < 350 Da (Fig. 4). CHO compounds with an MW > 500 Da were only detected in AS and AN (Fig. 4). Their carbon number was mostly below 20 in city samples, while compounds with ≥ C_{25} were detected under both airport conditions (see SI, Fig. S2). In the airport $PM_{2.5}$ samples we identified specific airport marker compounds which stem from pentaerythritol-based lubrication oils that have earlier been detected in ultrafine particles at the same site (*e.g.* $C_{25}H_{44}O_8$, level 1 and $C_{27}H_{48}O_8$, level 1) (Ungeheuer et al., 2021) (Fig. 4, circle 2). $C_{25}H_{44}O_8$ exhibited high sample-to-blank (s/b) ratios of up to 100 in AN and 68 in AS, while $C_{27}H_{48}O_8$ had s/b ratios of up to 40 in both AN and AS. Their occurrence during night-time was at the blank level for normal airport operation (AN27). Furthermore, we identified the compound $C_{16}H_{26}O_2$ in all samples as 4-*tert*-octylphenol monoethoxylate (OP1EO, level 2), a common environmental pollutant (Bergé et al., 2012; Renner, 1997; Ying et al., 2002). Its abundance was the highest in samples from the city condition (C4 and C5) and lowest in sample AN19. Moreover, caryophyllene oxide ($C_{15}H_{24}O$, level 2) was identified in AN, AS, and C with approximately the same averaged signal intensities.

In the class of CHN compounds, which largely represents amines and heterocyclic compounds, we observed 18 compounds across all samples. Thereof, 10 were found in AN, 11 in AS, and 17 in C. The summed signal intensity for all CHN compounds within AN and AS was at least twofold lower than in C but showed no significant differences between the sampling conditions. The predominant CHN compounds were similar within groups AN and AS and consisted mostly of cyclic amines, *e.g.*, norharmane ($C_{11}H_8N_2$, level 2), which was also found in C. Norharmane was most abundant in the samples C4 and AS31 (night). AN19 had the smallest signal and was approximately 20 times lower than C4.

The class of CHNO compounds consisted of 88 different compounds across all analysed samples whereof 76 were detected in the city group. In the groups AN and AS we detected 45 and 39 compounds, respectively. The summed signal intensities for C were significantly higher than those in AN ($p = 0.0130$) and AS ($p = 0.0261$), while AN and AS showed no significant difference (Fig. 6). The samples C4 and C5 had the largest overall signal intensity of CHNO compounds (Fig. 7). The lowest intensities were found in AN19 and AN24 (Fig. 7). The highest signals showed great heterogeneity among the sampling conditions, but none could be identified. However, many of the molecules were cyclic based on their H/C ratios of about 0.8 to 1.5. The largest measured CHNO signal was $C_{14}H_{21}NO$, which exhibited a fragment through the loss of C_3H_6. $C_{14}H_{21}NO$ was found in all groups and had about two- to threefold higher intensities in samples from the city wind-sector.

The class of CHOS compounds consisted of 19 different compounds across all samples. Thereof 11 were detected in C, 6 in AS, and 10 in AN. The largest signal areas of CHOS compounds were found in C3 and C7, the lowest in the night sample AN27. Notably, the highest CHOS signals for C consisted of smaller molecules with an MW < 300 Da while for AN and AS compounds with an MW > 450 Da were detected (Fig. 4). Their summed signal intensity was at least eightfold higher in C than in AN and AS. This could be traced back to a homologous row of four CHOS compounds ($C_{16}H_{16}OS$ to $C_{19}H_{22}OS$) present in C but absent in AS (Fig. 4, circle 3). Two of them ($C_{17}H_{18}OS$ and $C_{19}H_{22}OS$) were also found in AN but had at least sevenfold lower averaged signal intensities than in C. The homologues were characterised by their identical KMD of 0.19 Da and differed by a CH_2-unit (Fig. 4). The compounds could not be further identified with the mzcloud database, however, based on their H/C ratios of ~1 we can state that they likely contain a cyclic or unsaturated carbon skeleton.

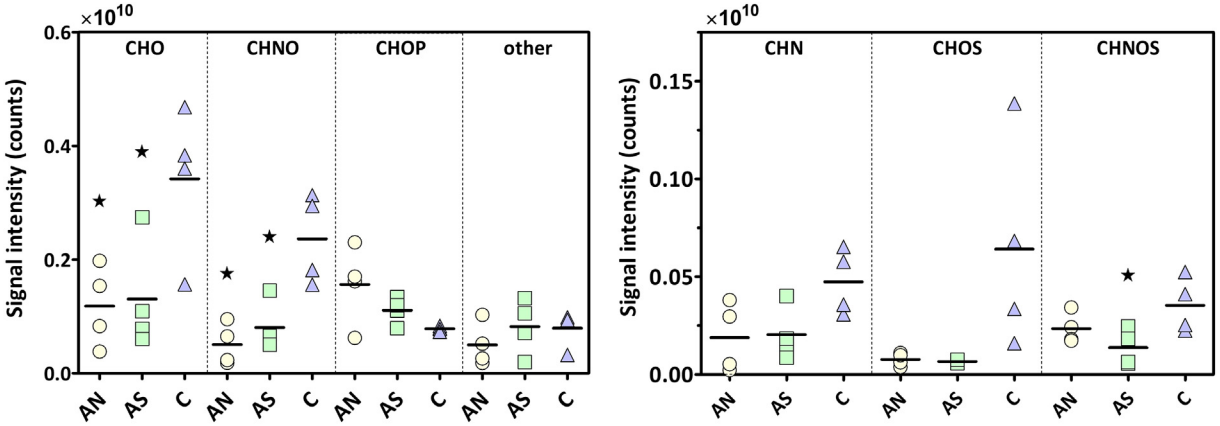

Fig. 6. Comparison between the summed signal intensities of the different compound classes. There were no significant differences between AN and AS. Significant differences between AN and AS against C with $p < 0.05$ are indicated by ★ (unpaired *t*-test with Welch's correction).

For the CHNOS class, 18 different signals were detected. Thereof, 11 were found in AN, 8 in AS, and 10 in C. Their summed signal intensity for C was significantly higher than for AS ($p = 0.0498$) (Fig. 6). Again, we observed the lowest summed signal intensities in the airport wind-sector (AN24 and AS29), and the highest for the city wind-sector (C5 and C4) (Fig. 7). One of the detected molecules was identified as the systemic herbicide prosulfocarb (PSC, $C_{14}H_{21}NOS$, level 1). PSC was present in all groups with the highest intensity in AN26 and C4 (Fig. 4). The night-time sample AS31 exhibited the lowest signal. Furthermore, the neurotoxic plasticiser N-butylbenzenesulfonamide ($C_{10}H_{15}NO_2S$, NBBS, level 2) (Rider et al., 2012) was identified in all samples from C, but it was largely absent in samples from the airport wind-sector (Fig. 4).

The class of CHOP compounds consisted of 29 different compounds across all samples. Thereof 17 compounds were detected in each AN and AS, and 21 compounds were found in C. We found that the CHOP-group is the only elemental composition group that exhibited the lowest summed intensity for samples from the city-sector. The AN samples were twofold higher than in C, and a third higher than in AS, indicating a strong emission of this class during normal airport operation. The compound $C_{12}H_{27}O_4P$ was identified as tributyl phosphate (TBP, level 1), which was absent in the city-sector and largely present in air masses from the airport during daytime with higher values under normal operating conditions and lower during the strike event (Fig. 4). Furthermore, we identified a homologous row of aromatic organophosphorus compounds ($C_{18}H_{15}O_4P$ to $C_{21}H_{21}O_4P$) based on a CH_2-based KMD, caused by the varying number of methylated phenyl groups (Fig. 4). The largest homologue was identified as tricresyl phosphate (TCP, level 1), which was absent in samples from the city sector and showed a lower averaged intensity under airport strike condition compared to the normal airport operation (Fig. 4). The highest signal of TCP was obtained during daytime and normal airport operation. The smallest homologue was identified as triphenyl phosphate (TPhP, level 1) and detected among all groups being at least sixfold higher on average in C than in AN and AS, indicating that this compound has other sources than the airport operation. The remaining two homologues $C_{20}H_{19}O_4P$ and $C_{19}H_{17}O_4P$ were also detected under all sampling conditions and were identified as dicresylphenyl- (DPP, level 1) and cresyldiphenyl phosphate (CDP, level 1). Both compounds were predominant in samples from the city condition. The compound $C_6H_{15}O_4P$ was identified as triethyl phosphate (TEP, level 1). TEP had the highest signal in C4 and had approximately two- to fivefold greater averaged signal intensities than in samples from AS and AN.

Contrasting the results of all sampling conditions, the non-target analysis revealed a greater heterogeneity regarding the organic aerosol composition for samples from the city centre wind-sector. We found a significantly larger signal intensity in samples from the city for the composition classes CHO, CHNO and CHNOS (Fig. 6). The CHOP class had the lowest signal intensity regarding samples from the city wind-sector. High molecular CHO compounds were only found in airport samples, while lower molecular compounds dominated in samples from C. Individual airport marker compounds, such as $C_{25}H_{44}O_8$, $C_{27}H_{48}O_8$, TCP, and TBP, were completely absent in the urban background aerosol under C-condition. Differences between both airport conditions were observable by the signal intensity of single compounds.

3.3. Correlation between in vitro inhibition, compound intensities and $PM_{2.5}$ mass concentration

We found a significant ($p < 0.01$) positive correlation between the inhibition of the highest used concentration in both *in vitro* assays (see 3.1.2

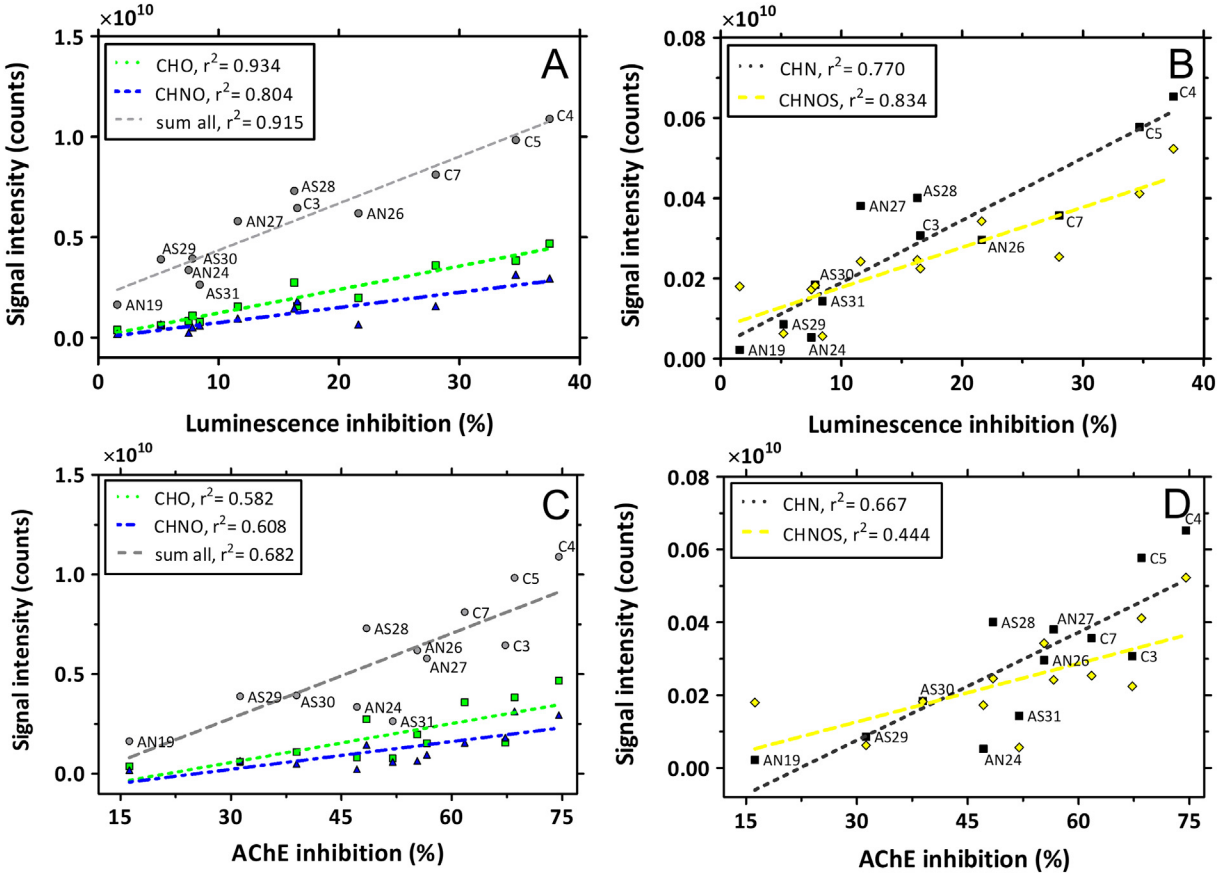

Fig. 7. Linear regression lines and coefficients of determination (r^2) for the correlation between the *in vitro* inhibition of the highest tested concentration and different compound classes. A – Linear regression lines and r^2 for CHO, CHNO and the sum of all compounds in the Microtox assay. B - Linear regression lines and r^2 for CHN and CHNOS compounds in the Microtox assay. C – Linear regression lines and r^2 for CHO, CHNO and the sum of all compounds in the AChE inhibition assay. D - Linear regression lines and r^2 for CHN and CHNOS compounds in the AChE inhibition assay.

AChE inhibition and SI, Fig. S3) and the summed signal intensity of organic aerosol compounds for four compound classes (CHO, CHN, CHNO, CHNOS) (Fig. 7). The highest coefficients of determination were found for the Microtox assay. The strongest correlation was found between the luminescence inhibition and signal intensity of the CHO compounds (r^2 = 0.934). This was followed by the correlation with the sum of all compounds (r^2 = 0.915), CHNOS (r^2 = 0.834), CHNO (r^2 = 0.804), and CHN compounds (r^2 = 0.770). The coefficients of determination were slightly lower for the comparison between AChE inhibition and different compound classes (Fig. 7). The sum of all compounds had the strongest correlation with AChE inhibition (r^2 = 0.682), CHNOS compounds the lowest (r^2 = 0.444).

We observed different organic composition classes, but certainly, a large fraction of $PM_{2.5}$ is not represented by our non-target analysis due to a specific extraction and ionisation method. However, we observed a strong correlation between the summed signal intensities of the detected organic molecules and averaged $PM_{2.5}$ mass concentration during the filter sampling periods (see SI, Fig. S4). Hence, we observe *in vitro* effects even at mass concentrations of 10 μg m^{-3} and less, as can be seen at sample C4, which exhibited the highest activity in both assays, although the average $PM_{2.5}$ mass concentration during this sampling interval was below 10 μg m^{-3}. Certainly, the transferability of these biological outcomes on human health effects is limited, but they can help identifying causal relationships between PM pollution and adverse health effects.

4. Discussion

4.1. Source attribution of single organic compounds

The chemical composition of the organic fraction in $PM_{2.5}$ determined by the non-target approach had a strong wind direction dependency. Possible emission sources of selected compounds are discussed in the following. The class of CHO compounds consisted of compounds with a molecular weight below 350 Da for samples from the city wind-sector, while compounds with a higher molecular weight were found in the airport wind-sector. The large CHO compounds $C_{25}H_{44}O_8$ and $C_{27}H_{48}O_8$ were only detected in airport samples (AN and AS). In an earlier work we examined ultrafine particles from the Frankfurt airport sampled at the same monitoring site and identified these compounds as pentaerythritol esters (PEEs) that are used in jet engine lubrication oils (Timko et al., 2010; Ungeheuer et al., 2021; Yu et al., 2012). This finding is supported by their absence under the city wind-sector condition and their high occurrence at the airport during the daytime. It remains ambiguous why we detect these compounds also in the night-time strike sample AS31. The emission of such jet oil constituents has previously been reported at other airports (Fushimi et al., 2019; Yu et al., 2012). The use of high molecular PEEs is especially reported for synthetic aviation oils, while oils used in automotive have an average MW of 340 Da (fresh) and 293 Da (used) (Chen et al., 1994; Vazquez-Duhalt, 1989). The substance 4-*tert*-octylphenol monoethoxylate (OP1EO) belongs to the class of alkylphenol ethoxylates (APEO). APEOs are the major group of non-ionic surfactants and have wide use as industrial cleaners, dispersing agents and emulsifiers, demulsifiers and solubilisers in agricultural products (Acir and Guenther, 2018; Ying et al., 2002). OP1EO is an environmental pollutant with endocrine disruption potential (Bergé et al., 2012; European Chemicals Agency (ECHA), 2020) and was predominantly detected in samples from the city wind-sector. The wide use of APEOs in cleaning and agricultural products makes them prone to high emissions from such environments as the city or nearby agricultural fields, which is why they are found ubiquitously in the environment, including the air (Bergé et al., 2012) This would explain the high occurrence of OP1EO in samples from the city condition. However, the compound also had high signal values in some airport samples.

The occurrence of the epoxide caryophyllene oxide showed no dependency of the wind-sector, yet airport samples tended to have higher signal intensities than city samples. Caryophyllene oxide is an oxidation product of β-caryophyllene that is naturally emitted by several plant families such as Pinaceae (Helmig et al., 2007; Pokorska et al., 2012; Sköld et al., 2006). Higher occurrences of caryophyllene oxide in samples from the south (airport wind-sector) can be explained by the biogenic emissions from the surrounding forest. Caryophyllene oxide is considered as an inhibitor of the mitochondrial electron transport chain (Monzote et al., 2009), however, its metabolites might exhibit different properties (Choudhary et al., 2006).

The cyclic amine norharmane had the highest abundance in C4, yet it was equally distributed among the remaining samples. Norharmane is a β-carboline and formed as a pyrolysis product in cooking and can be found in tobacco or marihuana smoke (Pfau and Skog, 2004; Rommelspacher et al., 2002). Pfau and Skog (2004) identified tobacco smoke as a major emission source. Reported emission index is ~12 μg norharmane g^{-1} tobacco (Poindexter and Carpenter, 1962; Rommelspacher et al., 2002). Therefore, high emissions around urban areas seem plausible. Nevertheless, this is contrasted by the further mentioned equal distribution between all samples except C4. A possible explanation is the sheer size of the Frankfurt Airport with plenty of restaurants and its large passenger numbers (potential smokers). Norharmane can induce neurodegeneration and motoric impairment (Östergren et al., 2006). It is further known as an inhibitor for the monoaminoxidase B and AChE (Rommelspacher et al., 2002; Skup et al., 1983).

NBBS is a neurotoxic plasticiser that is frequently used in polyacetals and polyamides (Rider et al., 2012). It is also naturally formed in greenhouse soil by the bacterium *Pseudomonas sp.* (Kim et al., 2000). Its abundance was high in the city samples C4 and C5 and low in samples taken under airport strike condition. This might be explained by the abrasion of brake pads. Polyamides such as Kevlar are used in brake and clutch pads due to their high-temperature resistance and solidity (Bin Kabir and Ferdous, 2012; Kankanala and Sarkar, 2020; Loken, 1980; Unaldi and Kus, 2014). Correspondingly, NBBS has already been described in particulate matter emissions from brake pads (Plachá et al., 2017). The city samples reflect an urban background with lots of motor traffic. Furthermore, its occurrence was slightly higher in samples taken during normal airport operation than during airport strike. This possibly reflects fewer breaking events due to the decreased airplane, shuttle, and passenger traffic.

PSC is a thiocarbamate herbicide and a relevant aerosol constituent with the potential to induce acute toxicity (Bo et al., 2020; Devault et al., 2019). Its wind-driven atmospheric dispersion is especially relevant in autumn with the highest described concentrations in November (Devault et al., 2019). Furthermore, the potential of long-range transport is described (Van Dijk and Guicherit, 1999). This corresponds with our unambiguous finding of PSC in $PM_{2.5}$ as the examined samples were sampled during November. Its occurrence could not be clearly assigned to a specific wind direction, which might be explained by its use. Agricultural fields are equally distributed among the sampled wind directions, so its abundance may rather depend on the seasonal application of PSC.

Most detected CHOP compounds can be attributed to the class of organophosphorus esters (OPEs). The OPEs identified on an identification confidence level of 1 included TCP, TBP, TPhP, CDP, DPP and TEP. OPEs are high-production-volume chemicals that are emitted into the environment by leaching and volatilisation (Marklund et al., 2003; Reemtsma et al., 2008). TBP was exclusively detected in samples from the airport. It is used as a plasticiser, anti-foaming agent, and additive in lubricants and hydraulic fluids (Marklund et al., 2005; Reemtsma et al., 2008). Marklund et al. (2005) examined OPE concentrations at the Umeå airport in Sweden and at a road intersection. They found TBP to be the most abundant of all measured OPEs at the airport. Its main source was identified as aircraft hydraulic fluids. Further, they did not find a strong correlation between TBP levels and road traffic (Marklund et al., 2005). This coincides with the finding that TBP had the highest signal intensity of all detected compounds and was only present in airport samples. The high abundance of TCP in airport samples can be explained by its distinctive use as an anti-wear agent in aircraft engine lubrication oils (de Boer et al., 2015; De Nola et al., 2008). Therefore, the TCP signals during the night-time flight ban at normal airport operation were remarkably lower than at daytime

and for the city condition, respectively. It further explained the lower average TCP signals during the airport strike. This is in accordance with previous examinations that described TCP as an airport marker compound (Fushimi et al., 2019; Ungeheuer et al., 2021). However, its high abundance during nighttime and strike (AS31) remains unclear. TCP acts as an inhibitor of acetylcholinesterase, its toxicity is dependent on the present isomers (Abou-Donia, 1981; Winder and Balouet, 2002). CDP, DPP, and TPhP had the highest abundances at wind directions from north-northeast to east-northeast (city). Because OPEs are not chemically bonded to the products they are used in, outgassing is likely to happen (Marklund et al., 2003; Rodríguez et al., 2006). Due to their ubiquitous use, large cities may have a higher burden than remote areas, thus explaining the lower occurrence of these compounds in airport samples. In contrast, Ren et al. (2016) reported significantly higher OPE concentrations in sub-urban air than in urban air. CDP and TPhP are used as flame retardants and plasticisers in PVC, hydraulic fluids, lubricants, electrical components, and the automobile industry (Esch et al., 1997; WHO & IPCS, 1991). CDP has already been found in indoor dust and soils (Björnsdotter et al., 2018; Huang et al., 2020; Wang et al., 2019). TPhP is a described endocrine disruptor and inhibits the acetylcholinesterase (Shi et al., 2018). TEP had a similar distribution behaviour between the sampling conditions as CDP and TPhP. It is also used as a flame retardant but does not inhibit the acetylcholinesterase (Gumbmann and Williams, 1970; Salthammer et al., 2003).

4.2. $PM_{2.5}$ composition and in vitro toxicity

The observed *in vitro* toxicity of the $PM_{2.5}$ filter extracts showed a strong wind direction dependency. Samples of the city wind-sector exhibited the highest toxicity, samples obtained during the airport strike event showed the lowest. The AChE assay assesses a characteristic mechanism for neurotoxicity from *i.e.*, organophosphorus compounds (Baron, 1981; Winder and Balouet, 2002) and revealed a higher sensitivity to the $PM_{2.5}$ extracts than the Microtox assay thus resulting in lower EC values. However, the inhibition of bioluminescence is a more sensitive indicator for unspecific toxicity than other assays such as mammalian cell viability assays (Neale et al., 2012). Both assays had a strong correlation with the total signal intensity of all detected organic compounds. The total signal intensities of the organic fraction also showed a strong correlation with the $PM_{2.5}$ mass concentration (SI, Fig. S4). Therefore, we also observe an apparent correlation between baseline toxicity/AChE inhibition and $PM_{2.5}$ mass concentration. This supports the need for low ambient $PM_{2.5}$ concentrations. Studies on the baseline toxicity of $PM_{2.5}$ are scarce. However, this explanation is following Lionetto et al. (2019) who examined the water-soluble fraction of urban PM_{10} with the Microtox assay. They found a positive correlation between the increase of luminescence inhibition and PM_{10} concentrations (Lionetto et al., 2019). Nonetheless, this contrasts with the findings of Roig et al. (2013). They found no correlation between the water-soluble fraction of PM_{10} and Microtox results. This was explained by varying PM_{10} compositions of which only a few compounds might induce toxicity (Roig et al., 2013). Considering that some samples had a high summed signal intensity but lower toxicity than samples with lower signal intensity, the chemical composition of $PM_{2.5}$ seems to play an important role. Further, both mentioned studies tested the water-soluble fraction of the coarse PM_{10} and measured its concentration. In contrast, the filters that we examined were extracted with an organic solvent, thus leading to a different extraction result. It can be assumed that highly lipophilic compounds have a higher extraction rate with an organic solvent such as the used DCM. Those differences make the comparison of different studies difficult. Yet $PM_{2.5}$ is reported to induce lower toxicity to *A. fischeri* than PM_{10} (Papadimitriou et al., 2006). This corresponds with the present results as reported Microtox EC_{50} values of PM_{10} (<20 m^3 air ml^{-1}) are lower than the obtained EC_{20} values of $PM_{2.5}$ (Roig et al., 2013). Roig et al. (2013) used acidified water, thus extracting a large amount of metals that might be more toxic and were not examined in this study. This suggests that the toxicity of PM depends on the specific sample composition and extracted compounds. To gain further insight on the effect of specific substances, substances with high signal intensities and described adverse effects were also tested for their correlation with the assay results (see SI, Table S3). OP1EO had a significant positive correlation with the results of both assays. Hence, it is a suspected driver of the found CHO compound dependent toxicity. The neurotoxicant norharmane also had a weak positive correlation with both assays, while NBBS only correlated with luminescence inhibition. The herbicide prosulfocarb had a significant positive correlation with both assays. Notably, no significant correlation between the sum of CHOP compounds and both assays was obtained. The CHOP class consisted of many OPEs that had the largest signals. As AChE inhibition is a specific mechanism of OPE toxicity (Eyer, 1995; Winder and Balouet, 2002), this finding was unexpected (see 4.3 Limitations). Therefore, the predominant OPEs were correlated with both assays, obtaining a positive correlation for TPhP, CDP, DPP and TEP (see SI, Table S3). TPhP is described as an AChE inhibitor (Shi et al., 2018). Therefore, a positive correlation between its abundance and the assay result is plausible. Interestingly, the signal intensities of TCP had no positive correlation with the inhibition of AChE. This might be an indicator for the use of nontoxic isomers in aircraft engine oils as the TCP-toxicity is strongly isomer-dependent (Eto et al., 1962; Winder and Balouet, 2002). This finding is in accordance with Ungeheuer et al. (2021) who reported the absence of the harmful tri-*ortho* isomer (TOCP) in aircraft engine lubrication oils and airport-related ultrafine particles.

4.3. Limitations

The toxicity of TOCP is described as dependent on its metabolic activation by the cytochrome P450 system (Eto et al., 1962), and might therefore be underestimated in this study. The activation leads to the formation of cyclic saligenin phosphate esters, which induce the toxic effect of TOCP (Eto et al., 1962; Lorke et al., 2016). This metabolic activation is also described for phosphorothioates and takes place in the brain, having a major role in acute toxicity (Sanchez-Hernandez and Walker, 2000). To address the metabolite-dependent toxicity of TCP, future studies with S9 liver extract, which mimics the hepatic metabolisation by P450 enzymes, are conceivable. We also observed a positive correlation between TEP and AChE inhibition, although it can be concluded that TEP is not responsible for the AChE inhibition as it has been evaluated as non-AChE inhibiting (Gumbmann and Williams, 1970). In contrast, TBP, which is described as AChE inhibitor had no significant correlation with the assay results. This might be explained by the exceeding effect of other neurotoxicants in the air masses from the city center. Therefore, these cases (TCP and TEP) point out the limitation of the correlation analysis. Based on the correlation analysis, we can only observe indications for potential drivers of toxicity, but cannot attribute the observed effects to individual compound classes or single compounds. An underlying hidden effect cannot be avoided when considering individual compound classes as only the whole filter extracts were analysed for *in vitro* toxicity. To overcome this limitation, future investigations shall apply fractionation of filter sample extracts before biotesting in order to clearly identify the key drivers of toxicity.

In our non-target analysis approach many detected compounds remain unidentified, and a part of the described compounds are only identified with an identification confidence of level 2 that is based on exact mass and fragmentation pattern comparison with a database. Future work is needed to unambiguously identify the suspected drivers of toxicity using authentic standards. However, the non-target analysis is a promising tool for holistic chemical characterisation of extracts of ambient PM.

The use of high-volume air samplers also holds the potential for sampling artifacts. The gas-particle partitioning of compounds is dependent on the temperature and the total suspended particles (Pankow, 1994). Volatile compounds can desorb from the filter depending on their physicochemical properties (Peters et al., 2000). This so-called 'blow-off' can take place during and after sampling. The potential desorption after sampling was addressed by the filter storage at −20 °C. The high volume flux of a high-volume air sampler may also lead to 'blow-on' events that increase the particle phase concentration (Peters et al., 2000). This is critical for organophosphorus compounds for which the gas-particle partitioning

behaviour is part of current research (Okeme et al., 2018). Furthermore, the used glass fiber filter material holds the potential of active zones, on which gaseous polar compounds might strongly adsorb.

5. Conclusions and outlook

In this study, we showed that the chemical composition and *in vitro* baseline toxicity and neurotoxicity of the organic fraction in urban background $PM_{2.5}$ strongly depends on the origin of the sampled air masses. The baseline toxicity and inhibition of acetylcholinesterase exhibited a strong correlation with the sum of the signals from (+)ESI-HRMS measurements of individual organic compounds. The sum of organic compounds also showed good correlation to the averaged $PM_{2.5}$ mass concentration. Considering the organic $PM_{2.5}$ fraction, the air mass advected from the urban city centre was found to be more toxic compared to the rural air from south-southwest carrying particle emissions from the airport. A minor difference between the toxicity of airport particle emissions of the strike event and of the normal operation was only found in the AChE inhibition assay. Based on the results, i.e. organophosphorus esters and the non-ionic surfactant OP1EO are suspected drivers of the AChE inhibition. The results indicate that the toxicity of the organic fraction in $PM_{2.5}$ is dependent on both its concentration and individual composition. This partially supports the need for low ambient $PM_{2.5}$ mass concentration, as recommended by the WHO. However, further work is necessary to (1) - comprehensively characterize the organic PM fraction with authentic standards, (2) identify the main drivers of toxicity as well as their metabolism-dependent toxicity, and (3) quantify the levels at which individual compounds pose a risk to human health. We recommend an approach by fractionating the samples and following an effect-directed analysis approach, including studies on the metabolic activation of single compounds or whole fractions. In parallel, the establishment of an atmospheric pollutants mass spectrometry database is urgently needed.

Financial support

This research has been supported by the Deutsche Forschungsgemeinschaft (DFG; German Research Foundation) (grant no. 410009325).

CRediT authorship contribution statement

Jonas P. Wallraff: Conceptualization, Formal analysis, Methodology, Investigation, Writing – original draft. **Florian Ungeheuer:** Methodology, Investigation, Supervision, Writing – review & editing. **Andrea Dombrowski:** Methodology, Writing – review & editing. **Jörg Oehlmann:** Resources, Supervision, Writing – review & editing. **Alexander L. Vogel:** Funding acquisition, Methodology, Resources, Software, Supervision, Writing – review & editing.

Declaration of competing interest

The authors declare that they have no competing financial interests or personal relationships that could have appeared to influence the work reported in this paper.

Acknowledgements

We thank Diana Rose, Florian Ditas, and Stefan Jacobi of the Hessian Agency for Nature Conservation, Environment and Geology for providing access to the air quality monitoring station, and acknowledge their provision of air quality data.

Appendix A. Supplementary data

Supplementary data to this article can be found online at https://doi.org/10.1016/j.scitotenv.2021.152779.

References

Abbas, M., Adil, M., Ehtisham-ul-Haque, S., Munir, B., Yameen, M., Ghaffar, A., Shar, G.A., Tahir, M.A., Iqbal, M., 2018. Vibrio fischeri bioluminescence inhibition assay for ecotoxicity assessment: a review. Sci. Total Environ. 626, 1295–1309. https://doi.org/10.1016/j.scitotenv.2018.01.066.

Abou-Donia, M.B., 1981. Organophosphorus ester-induced delayed neurotoxicity. Annu. Rev. Pharmacol. Toxicol. 21, 511–548. https://doi.org/10.1146/annurev.pa.21.040181.002455.

Acir, I.H., Guenther, K., 2018. Endocrine-disrupting metabolites of alkylphenol ethoxylates – a critical review of analytical methods, environmental occurrences, toxicity, and regulation. Sci. Total Environ. 635, 1530–1546. https://doi.org/10.1016/j.scitotenv.2018.04.079.

Arias-Pérez, R.D., Taborda, N.A., Gómez, D.M., Narvaez, J.F., Porras, J., Hernandez, J.C., 2020. Inflammatory effects of particulate matter air pollution. Environ. Sci. Pollut. Res. Int. 27, 42390–42404. https://doi.org/10.1007/s11356-020-10574-w.

Bandowe, B.A.M., Meusel, H., 2017. Nitrated polycyclic aromatic hydrocarbons (nitro-PAHs) in the environment – a review. Sci. Total Environ. 581–582, 237–257. https://doi.org/10.1016/j.scitotenv.2016.12.115.

Barnett, V., Lewis, T., 1994. Outliers in statistical data. 3rd ed. John Wiley & Sons, Chichester.

Baron, R.L., 1981. Delayed neurotoxicity and other consequences of organophosphate esters. Annu. Rev. Entomol. 26, 29–48. https://doi.org/10.1146/annurev.en.26.010181.000333.

Bates, J.T., Fang, T., Verma, V., Zeng, L., Weber, R.J., Tolbert, P.E., Abrams, J.Y., Sarnat, S.E., Klein, M., Mulholland, J.A., Russell, A.G., 2019. Review of acellular assays of ambient particulate matter oxidative potential: methods and relationships with composition, sources, and health effects. Environ. Sci. Technol. 53, 4003–4019. https://doi.org/10.1021/acs.est.8b03430.

Benson, R., 2009. Hazard to the developing male reproductive system from cumulative exposure to phthalate esters-dibutyl phthalate, diisobutyl phthalate, butylbenzyl phthalate, diethylhexyl phthalate, dipentyl phthalate, and diisononyl phthalate. Regul. Toxicol. Pharmacol. 53, 90–101. https://doi.org/10.1016/j.yrtph.2008.11.005.

Bergé, A., Cladière, M., Gasperi, J., Coursimault, A., Tassin, B., Moilleron, R., 2012. Meta-analysis of environmental contamination by alkylphenols. Environ. Sci. Pollut. Res. 19, 3798–3819. https://doi.org/10.1007/s11356-012-1094-7.

Bin Kabir, R., Ferdous, N., 2012. Kevlar the super tough fiber. Int. J. Text. Sci. 1, 78–83. https://doi.org/10.5923/j.textile.20120106.04.

Björnsdotter, M.K., Romera-García, E., Borrull, J., de Boer, J., Rubio, S., Ballesteros-Gómez, A., 2018. Presence of diphenyl phosphate and aryl-phosphate flame retardants in indoor dust from different microenvironments in Spain and the Netherlands and estimation of human exposure. Environ. Int. 112, 59–67. https://doi.org/10.1016/j.envint.2017.11.028.

Bo, X., Sun, J., Mei, Q., Wei, B., An, Z., Han, D., Li, Z., Xie, J., Zhan, J., He, M., 2020. Degradation of prosulfocarb by hydroxyl radicals in gas and aqueous phase: mechanisms, kinetics and toxicity. Ecotoxicol. Environ. Saf. 191, 110175. https://doi.org/10.1016/j.ecoenv.2020.110175.

de Boer, J., Antelo, A., van der Veen, I., Brandsma, S., Lammertse, N., 2015. Tricresyl phosphate and the aerotoxic syndrome of flight crew members current gaps in knowledge. Chemosphere 119, 58–61. https://doi.org/10.1016/j.chemosphere.2014.05.015.

Brack, W., 2003. Effect-directed analysis: a promising tool for the identification of organic toxicants in complex mixtures? Anal. Bioanal. Chem. 377, 397–407. https://doi.org/10.1007/s00216-003-2139-z.

Cassee, F.R., Héroux, M.-E., Gerlofs-Nijland, M.E., Kelly, F.J., 2013. Particulate matter beyond mass: recent health evidence on the role of fractions, chemical constituents and sources of emission. Inhal. Toxicol. 25, 802–812. https://doi.org/10.3109/08958378.2013.850127.

Chen, C.S.H., Delfino, J.J., Rao, P.S.C., 1994. Partitioning of organic and inorganic components from motor oil into water. Chemosphere 28, 1385–1400. https://doi.org/10.1016/0045-6535(94)90080-9.

Chew, S., Kolosowska, N., Saveleva, L., Malm, T., Kanninen, K.M., 2020. Impairment of mitochondrial function by particulate matter: implications for the brain. Neurochem. Int. 135, 104694. https://doi.org/10.1016/j.neuint.2020.104694.

Choudhary, M.I., Siddiqui, Z.A., Nawaz, S.A., Atta-ur-Rahman, 2006. Microbial transformation and butyrylcholinesterase inhibitory activity of (-)-caryophyllene oxide and its derivatives. J. Nat. Prod. 69, 1429–1434. https://doi.org/10.1021/np0680174.

Cronin, M.T.D., Schultz, T.W., 1998. Structure-toxicity relationships for three mechanisms of action of toxicity to Vibrio fischeri. Ecotoxicol. Environ. Saf. 39, 65–69. https://doi.org/10.1006/eesa.1997.1618.

Daellenbach, K.R., Uzu, G., Jiang, J., Cassagnes, L.-E., Leni, Z., Vlachou, A., Stefenelli, G., Canonaco, F., Weber, S., Segers, A., Kuenen, J.J.P., Schaap, M., Favez, O., Albinet, A., Aksoyoglu, S., Dommen, J., Baltensperger, U., Geiser, M., El Haddad, I., Jaffrezo, J.-L., Prévôt, A.S.H., 2020. Sources of particulate-matter air pollution and its oxidative potential in Europe. Nature 587, 414–419. https://doi.org/10.1038/s41586-020-2902-8.

De Nola, G., Kibby, J., Mazurek, W., 2008. Determination of ortho-cresyl phosphate isomers of tricresyl phosphate used in aircraft turbine engine oils by gas chromatography and mass spectrometry. J. Chromatogr. A 1200, 211–216. https://doi.org/10.1016/j.chroma.2008.05.035.

Devault, D.A., Guillemin, J., Millet, M., Eymery, F., Hulin, M., Merlo, M., 2019. Prosulfocarb at center stage! Environ. Sci. Pollut. Res. https://doi.org/10.1007/s11356-019-06928-8.

Ellman, G.L., Courtney, K.D., Andres, V., Featherstone, R.M., 1961. A new and rapid colorimetric determination of acetylcholinesterase activity. Biochem. Pharmacol. 7, 88–95. https://doi.org/10.1016/0006-2952(61)90145-9.

Esch, G.J., WHO &amp, IPCS, 1997. Environmental Health Criteria 192 - Flame Retardants: A General Introduction. World Health Organization (WHO), Geneva.

Escher, B.I., Bramaz, N., Quayle, P., Rutishauser, S., Vermeirssen, E.L.M., 2008. Monitoring of the ecotoxicological hazard potential by polar organic micropollutants in sewage

treatment plants and surface waters using a mode-of-action based test battery. J. Environ. Monit. 10, 622–631. https://doi.org/10.1039/b800951a.
Escher, B.I., Allinson, M., Altenburger, R., Bain, P.A., Balaguer, P., Busch, W., Crago, J., Denslow, N.D., Dopp, E., Hilscherova, K., Humpage, A.R., Kumar, A., Grimaldi, M., Jayasinghe, B.S., Jarosova, B., Jia, A., Makarov, S., Maruya, K.A., Medvedev, A., Mehinto, A.C., Mendez, J.E., Poulsen, A., Prochazka, E., Richard, J., Schifferli, A., Schlenk, D., Scholz, S., Shiraishi, F., Snyder, S., Su, G., Tang, J.Y.M., Burg, B.Van, Der, Linden, Der, S.C.V., Werner, I., Westerheide, S.D., Wong, C.K.C., Yang, M., Yeung, B.H.Y., Zhang, X., Leusch, F.D.L., 2014. Benchmarking organic micropollutants in wastewater, recycled water and drinking water with in vitro bioassays. Environ. Sci. Technol. 48, 1940–1956. https://doi.org/10.1021/es403899t.
Eto, M., Casida, J.E., Eto, T., 1962. Hydroxylation and cyclization reactions involved in the metabolism of tri-o-cresyl phosphate. Biochem. Pharmacol. 11, 337–352. https://doi.org/10.1016/0006-2952(62)90056-4.
European Chemicals Agency (ECHA), 2020. 2-[4-(1,1,3,3-Tetramethylbutyl)phenoxy]ethanol [WWW Document]. https://echa.europa.eu/substance-information/-/substanceinfo/100.150.206. (Accessed 26 February 2021).
European Environment Agency (EEA), 2019. Healthy Environment, Healthy Lives: How the Environment Influences Health and Well-being in Europe. https://doi.org/10.2800/53670 Denmark.
Eyer, P., 1995. Neuropsychopathological changes by organophosphorus compounds - a review. Hum. Exp. Toxicol. 14, 857–864. https://doi.org/10.1177/096032719501401101.
Fraport, 2020. Fraport-Verkehrszahlen 2019: Über 70,5 Millionen Passagiere am Flughafen Frankfurt [WWW Document]. https://www.fraport.com/de/newsroom/pressemitteilungen/2020/q1-2020/fraport-verkehrszahlen-2019–ueber-70-5-millionen-passagiere-am-.html. (Accessed 7 July 2021).
Fushimi, A., Saitoh, K., Fujitani, Y., Takegawa, N., 2019. Identification of jet lubrication oil as a major component of aircraft exhaust nanoparticles. Atmos. Chem. Phys. 19, 6389–6399. https://doi.org/10.5194/acp-19-6389-2019.
Gumbmann, M.R., Williams, S.N., 1970. Anticholinesterase activity of triethyl phosphate resulting from an impurity. J. Agric. Food Chem. 18, 76–77. https://doi.org/10.1021/jf60167a009.
Guo, Y., Wu, K., Huo, X., Xu, X., 2011. Sources, distribution, and toxicity of polycyclic aromatic hydrocarbons. J. Environ. Health 73, 22–25. https://doi.org/10.5772/10045.
Helmig, D., Ortega, J., Duhl, T., Tanner, D., Guenther, A., Harley, P., Wiedinmyer, C., Milford, J., Sakulyanontvittaya, T., 2007. Sesquiterpene emissions from pine trees - identifications, emission rates and flux estimates for the contiguous United States. Environ. Sci. Technol. 41, 1545–1553. https://doi.org/10.1021/es0618907.
Hermens, J., Busser, F., Leeuwangh, P., Musch, A., 1985. Quantitative structure-activity relationships and mixture toxicity of organic chemicals in photobacterium phosphoreum: the microtox test. Ecotoxicol. Environ. Saf. 9, 17–25. https://doi.org/10.1016/0147-6513(85)90030-2.
HLNUG, 2018. 1. Zwischenbericht zur Untersuchung der regionalen Luftqualität auf ultrafeine Partikel im Bereich des Flughafens Frankfurt. Wiesbaden.
HLNUG, 2019. Measurement Data Portal [WWW Document]. https://www.hlnug.de/messwerte/datenportal/messstelle/2/1/0619. (Accessed 7 July 2021).
Huang, Y., Tan, H., Li, L., Yang, L., Sun, F., Li, J., Gong, X., Chen, D., 2020. A broad range of organophosphate tri- and di-esters in house dust from Adelaide, South Australia: concentrations, compositions, and human exposure risks. Environ. Int. 142, 105872. https://doi.org/10.1016/j.envint.2020.105872.
ISO-Guideline 11348-3:2007, 2007. Water quality - determination of the inhibitory effect of water samples on the light emission of Vibrio fischeri (Luminescent bacteria test) - part 3: method using freeze-dried bacteria. https://doi.org/10.31030/1495363.
Kankanala, A.K., Sarkar, M., 2020. A review on material and wear analysis of automotive break pad. Int. Res. J. Eng. Technol. 7, 2537–2543. https://doi.org/10.1016/j.matpr.2018.10.114.
Kanninen, K.M., Lampinen, R., Rantanen, L.M., Odendaal, L., Jalava, P., Chew, S., White, A.R., 2020. Olfactory cell cultures to investigate health effects of air pollution exposure: implications for neurodegeneration. Neurochem. Int. 136, 104729. https://doi.org/10.1016/j.neuint.2020.104729.
Kendrick, E., 1963. A mass scale based on CH2 = 14.0000 for high resolution mass spectrometry of organic compounds. Anal. Chem. 35, 2146–2154. https://doi.org/10.1021/ac60206a048.
Kim, K.H., Jahan, S.A., Kabir, E., Brown, R.J.C., 2013. A review of airborne polycyclic aromatic hydrocarbons (PAHs) and their human health effects. Environ. Int. 60, 71–80. https://doi.org/10.1016/j.envint.2013.07.019.
Kim, K.K., Kang, J.G., Moon, S.S., Kang, K.Y., 2000. Isolation and identification of antifungal N-butylbenzenesulphonamide produced by pseudomonas sp. AB2. J. Antibiot. (Tokyo) 53, 131–136. https://doi.org/10.7164/antibiotics.53.131.
Landrigan, P.J., Fuller, R., Acosta, N.J.R., Adeyi, O., Arnold, R., Basu, N.N., Baldé, A.B., Bertollini, R., Bose-O'Reilly, S., Boufford, J.I., Breysse, P.N., Chiles, T., Mahidol, C., Coll-Seck, A.M., Cropper, M.L., Fobil, J., Fuster, V., Greenstone, M., Haines, A., Hanrahan, D., Hunter, D., Khare, M., Krupnick, A., Lanphear, B., Lohani, B., Martin, K., Mathiasen, K.V., McTeer, M.A., Murray, C.J.L., Ndahimananjara, J.D., Perera, F., Potočnik, J., Preker, A.S., Ramesh, J., Rockström, J., Salinas, C., Samson, L.D., Sandilya, K., Sly, P.D., Smith, K.R., Steiner, A., Stewart, R.B., Suk, W.A., van Schayck, O.C.P., Yadama, G.N., Yumkella, K., Zhong, M., 2018. The lancet commission on pollution and health. Lancet 391, 462–512. https://doi.org/10.1016/S0140-6736(17)32345-0.
Lelieveld, J., Evans, J.S., Fnais, M., Giannadaki, D., Pozzer, A., 2015. The contribution of outdoor air pollution sources to premature mortality on a global scale. Nature 525, 367–371. https://doi.org/10.1038/nature15371.
Lelieveld, J., Klingmüller, K., Pozzer, A., Pöschl, U., Fnais, M., Daiber, A., Münzel, T., 2019. Cardiovascular disease burden from ambient air pollution in Europe reassessed using novel hazard ratio functions. Eur. Heart J. 40, 1590–1596. https://doi.org/10.1093/eurheartj/ehz135.
Lim, S.S., Vos, T., Flaxman, A.D., Danaei, G., Shibuya, K., Adair-Rohani, H., Amann, M., Anderson, H.R., Andrews, K.G., Aryee, M., Atkinson, C., Bacchus, L.J., Bahalim, A.N., Balakrishnan, K., Balmes, J., Barker-Collo, S., Baxter, A., Bell, M.L., Blore, J.D., Blyth, F., Bonner, C., Borges, G., Bourne, R., Boussinesq, M., Brauer, M., Brooks, P., Bruce, N.G., Brunekreef, B., Bryan-Hancock, C., Bucello, C., Buchbinder, R., Bull, F., Burnett, R.T., Byers, T.E., Calabria, B., Carapetis, J., Carnahan, E., Chafe, Z., Charlson, F., Chen, H., Chen, J.S., Cheng, A.T.A., Child, J.C., Cohen, A., Colson, K.E., Cowie, B.C., Darby, S., Darling, S., Davis, A., Degenhardt, L., Dentener, F., Des Jarlais, D.C., Devries, K., Dherani, M., Ding, E.L., Dorsey, E.R., Driscoll, T., Edmond, K., Ali, S.E., Engell, R.E., Erwin, P.J., Fahimi, S., Falder, G., Farzadfar, F., Ferrari, A., Finucane, M.M., Flaxman, S., Fowkes, F.G.R., Freedman, G., Freeman, M.K., Gakidou, E., Ghosh, S., Giovannucci, E., Gmel, G., Graham, K., Grainger, R., Grant, B., Gunnell, D., Gutierrez, H.R., Hall, W., Hoek, H.W., Hogan, A., Hosgood, H.D., Hoy, D., Hu, H., Hubbell, B.J., Hutchings, S.J., Ibeanusi, S.E., Jacklyn, G.L., Jasrasaria, R., Jonas, J.B., Kan, H., Kanis, J.A., Kassebaum, N., Kawakami, N., Khang, Y.H., Khatibzadeh, S., Khoo, J.P., Kok, C., Laden, F., Lalloo, R., Lan, Q., Lathlean, T., Leasher, J.L., Leigh, J., Li, Y., Lin, J.K., Lipshultz, S.E., London, S., Lozano, R., Lu, Y., Mak, J., Malekzadeh, R., Mallinger, L., Marcenes, W., March, L., Marks, R., Martin, R., McGale, P., McGrath, J., Mehta, S., Mensah, G.A., Merriman, T.R., Micha, R., Michaud, C., Mishra, V., Hanafiah, K.M., Mokdad, A.A., Morawska, L., Mozaffarian, D., Murphy, T., Naghavi, M., Neal, B., Nelson, P.K., Nolla, J.M., Norman, R., Olives, C., Omer, S.B., Orchard, J., Osborne, R., Ostro, B., Page, A., Pandey, K.D., Parry, C.D.H., Passmore, E., Patra, J., Pearce, N., Pelizzari, P.M., Petzold, M., Phillips, M.R., Pope, D., Pope, C.A., Powles, J., Rao, M., Razavi, H., Rehfuess, E.A., Rehm, J.T., Ritz, B., Rivara, F.P., Roberts, T., Robinson, C., Rodriguez-Portales, J.A., Romieu, I., Room, R., Rosenfeld, L.C., Roy, A., Rushton, L., Salomon, J.A., Sampson, U., Sanchez-Riera, L., Sanman, E., Sapkota, A., Seedat, S., Shi, P., Shield, K., Shivakoti, R., Singh, G.M., Sleet, D.A., Smith, E., Smith, K.R., Stapelberg, N.J.C., Steenland, K., Stöckl, H., Stovner, L.J., Straif, K., Straney, L., Thurston, G.D., Tran, J.H., Van Dingenen, R., Van Donkelaar, A., Veerman, J.L., Vijayakumar, L., Weintraub, R., Weissman, M.M., White, R.A., Whiteford, H., Wiersma, S.T., Wilkinson, J.D., Williams, H.C., Williams, W., Wilson, N., Woolf, A.D., Yip, P., Zielinski, J.M., Lopez, A.D., Murray, C.J.L., Ezzati, M., 2012. A comparative risk assessment of burden of disease and injury attributable to 67 risk factors and risk factor clusters in 21 regions, 1990–2010: a systematic analysis for the global burden of disease study 2010. Lancet 380, 2224–2260. https://doi.org/10.1016/S0140-6736(12)61766-8.
Lionetto, M.G., Guascito, M.R., Caricato, R., Giordano, M.E., De Bartolomeo, A.R., Romano, M.P., Conte, M., Dinoi, A., Contini, D., 2019. Correlation of oxidative potential with ecotoxicological and cytotoxicological potential of PM10 at an urban background site in Italy. Atmosphere (Basel). 10. https://doi.org/10.3390/ATMOS10120733.
Loken, H.Y., 1980. Asbestos free brakes and dry clutches reinforced with Kevlar® aramid fiber. SAE Tech. Pap. 89, 2202–2208. https://doi.org/10.4271/800667.
Lorke, D.E., Stegmeier-Petroianu, A., Petroianu, G.A., 2016. Biologic activity of cyclic and caged phosphates: a review. J. Appl. Toxicol. 37, 13–22. https://doi.org/10.1002/jat.3369.
Marklund, A., Andersson, B., Haglund, P., 2003. Screening of organophosphorus compounds and their distribution in various indoor environments. Chemosphere 53, 1137–1146. https://doi.org/10.1016/S0045-6535(03)00666-0.
Marklund, A., Andersson, B., Haglund, P., 2005. Traffic as a source of organophosphorus flame retardants and plasticizers in snow. Environ. Sci. Technol. 39, 3555–3562. https://doi.org/10.1021/es0482177.
Monzote, L., Stamberg, W., Staniek, K., Gille, L., 2009. Toxic effects of carvacrol, caryophyllene oxide, and ascaridole from essential oil of Chenopodium ambrosioides on mitochondria. Toxicol. Appl. Pharmacol. 240, 337–347. https://doi.org/10.1016/j.taap.2009.08.001.
Neale, P.A., Antony, A., Bartkow, M.E., Farré, M.J., Heitz, A., Kristiana, I., Tang, J.Y.M., Escher, B.I., 2012. Bioanalytical assessment of the formation of disinfection byproducts in a drinking water treatment plant. Environ. Sci. Technol. 46, 10317–10325. https://doi.org/10.1021/es302126t.
Okeme, J.O., Rodgers, T.F.M., Jantunen, L.M., Diamond, M.L., 2018. Examining the gas-particle partitioning of organophosphate esters: how reliable are air measurements? Environ. Sci. Technol. 52, 13834–13844. https://doi.org/10.1021/acs.est.8b04588.
Östergren, A., Fredriksson, A., Brittebo, E.B., 2006. Norharman-induced motoric impairment in mice: neurodegeneration and glial activation in substantia nigra. J. Neural Transm. 113, 313–329. https://doi.org/10.1007/s00702-005-0334-0.
Pankow, J.F., 1994. An absorption model of gas/particle partitioning of organic compounds in the atmosphere. Atmos. Environ. 28, 185–188. https://doi.org/10.1016/1352-2310(94)90093-0.
Papadimitriou, C., Evagelopoulos, V., Samaras, P., Triantafyllou, A.G., Zoras, S., Albanis, T.A., 2006. Toxicity of atmospheric particulate matter using aquatic bioassays. WIT Trans. Biomed. Health 10, 31–39. https://doi.org/10.2495/ETOX060041.
Peters, A.J., Lane, D.A., Gundel, L.A., Northcott, G.L., Jones, K.C., 2000. A comparison of high volume and diffusion denuder samplers for measuring semivolatile organic compounds in the atmosphere. Environ. Sci. Technol. 34, 5001–5006. https://doi.org/10.1021/es000056t.
Peters, R., Ee, N., Peters, J., Booth, A., Mudway, I., Anstey, K.J., 2019. Air pollution and dementia: a systematic review. J. Alzheimers Dis. 70, S145–S163. https://doi.org/10.3233/JAD-180631.
Pfau, W., Skog, K., 2004. Exposure to β-carbolines norharman and harman. JChromatogr. B Anal. Technol. Biomed. Life Sci. 802, 115–126. https://doi.org/10.1016/j.jchromb.2003.10.044.
Plachá, D., Vaculík, M., Mikeska, M., Dutko, O., Peikertová, P., Kukutschová, J., Mamulová Kutláková, K., Růžičková, J., Tomášek, V., Filip, P., 2017. Release of volatile organic compounds by oxidative wear of automotive friction materials. Wear 376–377, 705–716. https://doi.org/10.1016/j.wear.2016.12.016.

Poindexter, E.H., Carpenter, R.D., 1962. The isolation of harmane and norharmane from tobacco and cigarette smoke. Phytochemistry 1, 215–221. https://doi.org/10.1016/S0031-9422(00)82825-3.

Pokorska, O., Dewulf, J., Amelynck, C., Schoon, N., Šimpraga, M., Steppe, K., Van Langenhove, H., 2012. Isoprene and terpenoid emissions from Abies alba: identification and emission rates under ambient conditions. Atmos. Environ. 59, 501–508. https://doi.org/10.1016/j.atmosenv.2012.04.061.

Reemtsma, T., García-López, M., Rodríguez, I., Quintana, J.B., Rodil, R., 2008. Organophosphorus flame retardants and plasticizers in water and air IOccurrence and fate. Trends Anal. Chem. 27, 727–737. https://doi.org/10.1016/j.trac.2008.07.002.

Ren, G., Chen, Z., Feng, J., Ji, W., Zhang, J., Zheng, K., Yu, Z., Zeng, X., 2016. Organophosphate esters in total suspended particulates of an urban city in East China. Chemosphere 164, 75–83. https://doi.org/10.1016/j.chemosphere.2016.08.090.

Renner, R., 1997. European bans on surfactant trigger transatlantic debate. Environ. Sci. Technol. 31. https://doi.org/10.1021/es972366q.

Rider, C.V., Janardhan, K.S., Rao, D., Morrison, J.P., McPherson, C.A., Harry, G.J., 2012. Evaluation of N-butylbenzenesulfonamide (NBBS) neurotoxicity in Sprague-dawley male rats following 27-day oral exposure. Neurotoxicology 33, 1528–1535. https://doi.org/10.1016/j.neuro.2012.07.002.

Rodríguez, I., Calvo, F., Quintana, J.B., Rubí, E., Rodil, R., Cela, R., 2006. Suitability of solid-phase microextraction for the determination of organophosphate flame retardants and plasticizers in water samples. J. Chromatogr. A 1108, 158–165. https://doi.org/10.1016/j.chroma.2006.01.008.

Roig, N., Sierra, J., Rovira, J., Schuhmacher, M., Domingo, J.L., Nadal, M., 2013. In vitro tests to assess toxic effects of airborne PM10 samples. Correlation with metals and chlorinated dioxins and furans. Sci. Total Environ. 443, 791–797. https://doi.org/10.1016/j.scitotenv.2012.11.022.

Rommelspacher, H., Meier-Henco, M., Smolka, M., Kloft, C., 2002. The levels of norharman are high enough after smoking to affect monoamineoxidase B in platelets. Eur. J. Pharmacol. 441, 115–125. https://doi.org/10.1016/S0014-2999(02)01452-8.

Rönkkö, T.J., Hirvonen, M.-R., Happo, M.S., Ihantola, T., Hakkarainen, H., Martikainen, M.-V., Gu, C., Jokiniemi, J., Komppula, M., Jalava, P.I., Wang, Q.'.G., 2021. Inflammatory responses of urban air PM modulated by chemical composition and different air quality situations in Nanjing, China. Environ. Res. 192, 110382. https://doi.org/10.1016/j.envres.2020.110382.

Salthammer, T., Fuhrmann, F., Uhde, E., 2003. Flame retardants in the indoor environment - part II: release of VOCs (triethylphosphate and halogenated degradation products) from polyurethane. Indoor Air 13, 49–52. https://doi.org/10.1034/j.1600-0668.2003.01150.x.

Sanchez-Hernandez, J.C., Walker, C.H., 2000. In vitro and in vivo cholinesterase inhibition in lacertides by phosphonate- and phosphorothioate-type organophosphates. Pestic. Biochem. Physiol. 67, 1–12. https://doi.org/10.1006/pest.1999.2471.

Schraufnagel, D.E., 2020. The health effects of ultrafine particles. Exp. Mol. Med. 52, 311–317. https://doi.org/10.1038/s12276-020-0403-3.

Schraufnagel, D.E., Balmes, J.R., de Matteis, S., Hoffman, B., Kim, W.J., Perez-Padilla, R., Rice, M., Sood, A., Vanker, A., Wuebbles, D.J., 2019. Health benefits of air pollution reduction. Ann. Am. Thorac. Soc. 16, 1478–1487. https://doi.org/10.1513/AnnalsATS.201907-538CME.

Schultz, T.W., Cronin, M.T.D., 1997. Quantitative structure-activity relationships for weak acid respiratory uncouplers to Vibrio fisheri. Environ. Toxicol. Chem. 16, 357–360. https://doi.org/10.1897/1551-5028(1997)016<0357:QSARFW>2.3.CO;2.

Schymanski, E.L., Jeon, J., Gulde, R., Fenner, K., Ruff, M., Singer, H.P., Hollender, J., 2014. Identifying small molecules via high resolution mass spectrometry: communicating confidence. Environ. Sci. Technol. 48, 2097–2098. https://doi.org/10.1021/es5002105.

Shi, Q., Wang, M., Shi, F., Yang, L., Guo, Y., Feng, C., Liu, J., Zhou, B., 2018. Developmental neurotoxicity of triphenyl phosphate in zebrafish larvae. Aquat. Toxicol. 203, 80–87. https://doi.org/10.1016/j.aquatox.2018.08.001.

Sigma-Aldrich, 2018. Acetylcholinesterase Inhibitor Screening Kit MAK324 - Technical Bulletin [WWW Document]. . https://www.sigmaaldrich.com/deepweb/assets/sigmaaldrich/product/documents/370/429/mak324bul.pdf. (Accessed 6 June 2020).

Sköld, M., Karlberg, A.T., Matura, M., Börje, A., 2006. The fragrance chemical β-caryophyllene - air oxidation and skin sensitization. Food Chem. Toxicol. 44, 538–545. https://doi.org/10.1016/j.fct.2005.08.028.

Skup, M., Oderfeld-Nowak, B., Rommelspacher, H., 1983. In vitro studies on the effect of β-carbolines on the activities of acetylcholinesterase and choline acetyltransferase and on the muscarinic receptor binding of the rat brain. J. Neurochem. 41, 62–68. https://doi.org/10.1111/j.1471-4159.1983.tb11814.x.

Timko, M.T., Onash, T.B., Northway, M.J., Jayne, J.T., Canagaratna, M.R., Herndon, S.C., Wood, E.C., Miake-Lye, R.C., 2010. Gas turbine engine emissions — part II: chemical properties of particulate matter. J. Eng. Gas Turbines Power 132, 1–15. https://doi.org/10.1115/1.4000132.

UBA (Umweltbundesamt), 2004. Umwelt-Survey 1998 Band V: Hausstaub. Berlin.

UBA (Umweltbundesamt), 2017. Frequently Asked Questions About Phthalates and Plasticisers [WWW Document]. https://bit.ly/3jrDejq. (Accessed 8 May 2021).

Unaldi, M., Kus, R., 2014. Effect of pressing pressure on density and hardness of powder miscanthus reinforced brake pads. Appl. Mech. Mater. 680, 237–240. https://doi.org/10.4028/www.scientific.net/AMM.680.237.

Ungeheuer, F., van Pinxteren, D., Vogel, A.L., 2021. Identification and source attribution of organic compounds in ultrafine particles near Frankfurt international airport. Atmos. Chem. Phys. 21, 3763–3775. https://doi.org/10.5194/acp-21-3763-2021.

Van Dijk, H.F.G., Guicherit, R., 1999. Atmospheric dispersion of current-use pesticides: A review of the evidence from monitoring studies. Air. Soil Pollut, Water https://doi.org/10.1023/A:1005293020536.

Vazquez-Duhalt, R., 1989. Environmental impact of used motor oil. Sci. Total Environ. 79, 1–23. https://doi.org/10.1016/0048-9697(89)90049-1.

Vogel, A.L., Lauer, A., Fang, L., Arturi, K.R., Bachmeier, F., Dällenbach, K.R., Käser, T., Vlachou, A., Pospisilova, V., Baltensperger, U., El Haddad, I., Schwikowski, M., Bjelić, S., 2019. A comprehensive nontarget analysis for the molecular reconstruction of organic aerosol composition from glacier ice cores. Environ. Sci. Technol. 53, 12565–12575. https://doi.org/10.1021/acs.est.9b03091.

Völker, J., Vogt, T., Castronovo, S., Wick, A., Ternes, T.A., Joss, A., Oehlmann, J., Wagner, M., 2017. Extended anaerobic conditions in the biological wastewater treatment: higher reduction of toxicity compared to target organic micropollutants. Water Res. 116, 220–230. https://doi.org/10.1016/j.watres.2017.03.030.

Wang, Y., Yao, Y., Li, W., Zhu, H., Wang, L., Sun, H., Kannan, K., 2019. A nationwide survey of 19 organophosphate esters in soils from China: spatial distribution and hazard assessment. Sci. Total Environ. 671, 528–535. https://doi.org/10.1016/j.scitotenv.2019.03.335.

WHO, 2021. WHO global air quality guidelines. Particulate matter (PM2.5 and PM10), ozone, nitrogen dioxide, sulfur dioxide and carbon monoxide. 2021. World Health Organization, Geneva Licence: CC BY-NC-SA 3.0 IGO.

WHO &amp, IPCS, 1991. Environmental Health Criteria 111: Triphenyl Phosphate. World Health Organization (WHO), Vammala.

Winder, C., Balouet, J.C., 2002. The toxicity of commercial jet oils. Environ. Res. 89, 146–164. https://doi.org/10.1006/enrs.2002.4346.

Wong, F., de Wit, C.A., Newton, S.R., 2018. Concentrations and variability of organophosphate esters, halogenated flame retardants, and polybrominated diphenyl ethers in indoor and outdoor air in StockholmSweden. Environ. Pollut. 240, 514–522. https://doi.org/10.1016/j.envpol.2018.04.086.

Xing, Y.F., Xu, Y.H., Shi, M.H., Lian, Y.X., 2016. The impact of PM2.5 on the human respiratory system. J. Thorac. Dis. 8, 69–74. https://doi.org/10.3978/j.issn.2072-1439.2016.01.19.

Ying, G.G., Williams, B., Kookana, R., 2002. Environmental fate of alkylphenols and alkylphenol ethoxylates - a review. Environ. Int. 28, 215–226. https://doi.org/10.1016/S0160-4120(02)00017-X.

Yu, Z., Herndon, S.C., Ziemba, L.D., Timko, M.T., Liscinsky, D.S., Anderson, B.E., Miake-Lye, R.C., 2012. Identification of lubrication oil in the particulate matter emissions from engine exhaust of in-service commercial aircraft. Environ. Sci. Technol. 46, 9630–9637. https://doi.org/10.1021/es301692t.

Zhou, L., Hiltscher, M., Gruber, D., Püttmann, W., 2017. Organophosphate flame retardants (OPFRs) in indoor and outdoor air in the Rhine/Main area, Germany: comparison of concentrations and distribution profiles in different microenvironments. Environ. Sci. Pollut. Res. 24, 10992–11005. https://doi.org/10.1007/s11356-016-6902-z.